THE ATOMKI ANOMALY IN THE FRAMEWORK OF EXTENDED TWO-HIGGS-DOUBLET MODELS

A THESIS SUBMITTED TO
THE GRADUATE SCHOOL OF NATURAL AND APPLIED SCIENCES
OF
MIDDLE EAST TECHNICAL UNIVERSITY

BY

ZOZAN SARI

IN PARTIAL FULFILLMENT OF THE REQUIREMENTS
FOR
THE DEGREE OF MASTER OF SCIENCE
IN
PHYSICS

SEPTEMBER 2024

Approval of the thesis:

THE ATOMKI ANOMALY IN THE FRAMEWORK OF EXTENDED TWO-HIGGS-DOUBLET MODELS

submitted by **ZOZAN SARI** in partial fulfillment of the requirements for the degree of **Master of Science in Physics Department, Middle East Technical University** by,

Prof. Dr. Naci Emre Altun
Dean, Graduate School of **Natural and Applied Sciences** _____

Prof. Dr. Seçkin Kürkçüoğlu
Head of Department, **Physics** _____

Prof. Dr. İsmail Turan
Supervisor, **Physics, METU** _____

Examining Committee Members:

Prof. Dr. Tahmasib Aliyev
Physics, METU _____

Prof. Dr. İsmail Turan
Physics, METU _____

Assoc. Prof. Dr. Levent Selbuz
Physics Engineering, Ankara University _____

Date: 06.09.2024

I hereby declare that all information in this document has been obtained and presented in accordance with academic rules and ethical conduct. I also declare that, as required by these rules and conduct, I have fully cited and referenced all material and results that are not original to this work.

Name, Surname: Zozan Sarı

Signature :

ABSTRACT

THE ATOMKI ANOMALY IN THE FRAMEWORK OF EXTENDED TWO-HIGGS-DOUBLET MODELS

Sarı, Zozan
M.S., Department of Physics
Supervisor: Prof. Dr. İsmail Turan

September 2024, 55 pages

In 2016, the ATOMKI collaboration observed an anomaly in the decay of the excited beryllium atoms. This anomaly indicates the possible existence of a 17 MeV particle. Even though there has been no independent verification of the results yet, it is still worthwhile to discuss possible scenarios explaining the Atomki anomaly, which might put further constraints on the so-called hidden/dark sector physics. In this thesis, an extended two-Higgs-doublet model will be examined, incorporating existing constraints from various other experiments to address this anomaly.

Keywords: 2HDM, ATOMKI, Beryllium Anomaly, X17, BSM

ÖZ

GENİŞLETİLMİŞ İKİ HİGGS DUBLET MODELLERİ ÇERÇEVESİNDE ATOMKI ANOMALİSİ

Sarı, Zozan
Yüksek Lisans, Fizik Bölümü
Tez Yöneticisi: Prof. Dr. İsmail Turan

Eylül 2024 , 55 sayfa

2016 yılında ATOMKI işbirliği uyarılmış berilyum atomlarının bozunumunda bir anomali gözlemledi. Bu anomali olası bir 17 MeV kütleli parçacığın varlığına işaret ediyor. Her ne kadar sonuçlar henüz bağımsız olarak doğrulanmamış olsa da gizli/karanlık sektör fiziğine getireceği ilave sınırlar sebebiyle ATOMKI anomalisini tartışmak faydalı olacaktır. Bu tezde, bu anomali genişletilmiş iki Higgs dublet modeliyle, diğer çeşitli deneylerden elde edilen mevcut kısıtlamalar da dikkate alınarak incelenecektir.

Anahtar Kelimeler: 2HDM, ATOMKI, Berilyum Anomalisi, X17, SMÖ

To my family

ACKNOWLEDGMENTS

First and foremost, I would like to express my deepest gratitude to my supervisor, Prof. Dr. İsmail Turan, for his invaluable guidance and support throughout my master's study.

I would also like to thank Altuğ Elpe for his support and help throughout this thesis study. His contribution was key in completing this work.

I like to extend my heartfelt thanks to my friends for always being there when I needed them and supporting me in every possible way. Their constant encouragement and understanding have meant the world to me throughout this journey.

I am also incredibly thankful to my family for their unconditional love, patience, and encouragement.

Lastly, I would like to acknowledge TÜBİTAK for awarding me the 2210 scholarship.

TABLE OF CONTENTS

LIST OF TABLES

TABLES

LIST OF FIGURES

FIGURES

LIST OF ABBREVIATIONS

2HDM	Two Higgs Doublet Model
BSM	Beyond Standard Model
em	Electromagnetism
EW	Electroweak Theory
FCNC	Flavour Changing Neutral Currents
KM	Kinetic Mixing
NFC	Natural Flavour Conservation
QED	Quantum Electrodynamics
SM	Standard Model
SSB	Spontaneous Symmetry Breaking
vev	Vacuum Expectation Value

CHAPTER 1

INTRODUCTION

The Standard Model (SM) is a highly successful theory that accurately explains the fundamental building blocks of our universe. Nevertheless, it remains incomplete in addressing many fundamental questions. For instance, there are too many free parameters in SM that are determined solely through experiments. SM cannot answer why there is a predominance of matter over antimatter, the nature of dark energy and the composition of dark matter. Also, gravity is not included in the SM. It also fails to explain the strong CP problem and neutrino oscillations, and it cannot account for observed anomalies such as the muon anomalous magnetic moment. Such unresolved questions motivate physicists to explore the physics beyond the Standard Model (BSM).

In the quest to discover what is beyond SM, there are essentially three approaches: investigating heavy BSM particles at high energies using accelerators, known as energy frontier research; searching for lighter particles in low-energy, high-intensity experimental setups, referred to as intensity frontier research; and studying natural cosmic sources to uncover new, unknown particles, known as cosmic frontier research. An unidentified particle was detected in 2016 through intensity frontier research at a Hungarian accelerator facility.

In 2016, the ATOMKI collaboration reported an anomaly[6] now referred as the ATOMKI anomaly, Beryllium anomaly, or X17 anomaly. This anomaly was observed in the decay of the excited Beryllium atoms. They created excited beryllium atoms through the proton capture process; later, this excited state decays into its ground state by emitting an electron-positron pair. Their observation revealed a bump in the opening angle and the invariant mass of e^+e^- pair, showing a 6.8σ deviation in the angular

correlation. It was concluded that this anomaly is highly unlikely to be explained by the current understanding of nuclear physics. However, it could potentially be explained by introducing a new boson with a mass around 17 MeV. Later they improved their set-up and repeated their measurements using ^{4}He [9] [10] and ^{12}C [11] nuclei. Despite the improvements and use of different nuclei, the anomalous bump was still observed. To explain this anomaly, many theories have been proposed since it was observed.

In this thesis, this anomaly will be investigated and an explanation for it will be sought. A new abelian U(1) symmetry will be introduced to the SM symmetry group, and the scalar part of the SM will be extended by an additional Higgs doublet and a singlet. Right-handed neutrinos will also be introduced in the model to ensure it is anomaly-free. There are a number of two-Higgs-Doublet Models (2HDM) [12]. The specifics of our model will be provided.

The discovery of the Higgs boson was a significant success for the SM. However, the SM Higgs is a minimal theory and can be extended in various ways. 2HDMs offer a rich environment for the vacuum structure, providing many motivations to study 2HDMs. The most recognized motivation is supersymmetry [13], which incorporates two Higgs doublets in the Minimal Supersymmetric Standard Model. Other motivation arise from axion models [14][15] and baryogenesis[16].

In the Chapter 2, a summary of the SM is provided. The essential theoretical background needed to construct the model is presented in that chapter. In Chapter 3, the model is constructed, and the necessary parameters are calculated. In Chapter 4, the ATOMKI experiment is explained in detail, constraints from other experiments are listed, and a final analysis is conducted.

CHAPTER 2

THE STANDARD MODEL

The Standard Model (SM) is currently our most successful theory explaining the building blocks of matter and the forces of the universe. In this theory, the fundamental particles are classified into two categories: Spin half fermions, which constitute matter, and spin integer bosons, which mediate the forces. Fermions are also divided into two groups: quarks and leptons. There are six quarks and six leptons divided into three generations. Each generation differs only by their masses. Bosons are the particles exchanged between particles with non-zero quantum numbers, resulting in the forces we observe. Photons are exchanged in electromagnetic interactions between particles with electric charge; gluons are exchanged between coloured charges, which is the charge of the strong force; $W^{\pm}$ and Z bosons are involved in weak interactions; and finally, Higgs boson is what gives the mass of the particles. Table 2.1 summarizes these classifications.

In SM, interactions between quarks and leptons carried by bosons are described by the gauge group: $SU(3)_C \times SU(2)_L \times U(1)_Y$. The strong interactions are described

Table 2.1: The Standard Model particle content.

				BOSONS	
FERMIONS				Vector	Scalar
Quarks	u	c	t	γ	H
	d	s	b	g	
Leptons	e	μ	τ	$W^{\pm}$	
	ν_e	ν_μ	ν_τ	Z	

by $SU(3)_C$ group, and the electroweak interactions as a unified theory described by $SU(2)_L \times U(1)_Y$ group.

The model considered in this thesis is an extension to $SU(2)_L \times U(1)_Y$ and does not affect the strong interactions. Therefore, before introducing the framework of our model, the electroweak theory with spontaneous symmetry breaking will be elaborated in this chapter.

2.1 Quantum Electrodynamics

Quantum Electrodynamics (QED) is the quantum field theory of electromagnetic interactions, and electromagnetism is the easiest and the most familiar interaction of the SM. Therefore, it is a good starting point. This interaction arises from the abelian local $U(1)$ gauge invariance. The invariance of the Lagrangian of a free Dirac particle

$$\mathcal{L}_{Dirac} = \bar{\psi}(i\gamma^\mu \partial_\mu - m)\psi \tag{2.1}$$

transforming under local $U(1)$ symmetry,

$$\psi \to \psi' = e^{iq\alpha(x)}\psi \tag{2.2}$$

requires the introduction of the covariant derivative,

$$D_\mu \equiv \partial_\mu + iqA_\mu(x). \tag{2.3}$$

$A_\mu = (V(x), \mathbf{A}(x))$ is the electromagnetic vector potential where $\mathbf{E} = -\boldsymbol{\nabla} V - \partial_t \mathbf{A}$ and $\mathbf{B} = \boldsymbol{\nabla} \times \mathbf{A}$, q is the electric charge. Finally, transforming the vector potential,

$$A_\mu \to A'_\mu = A_\mu - \partial_\mu \alpha(x) \tag{2.4}$$

ensures the gauge invariance of $\mathcal{L}_{Dirac}$. After the introduction of the gauge field, which is the vector potential for the electromagnetic interaction, the Lagrangian become gauge invariant, but an extra term arises. It turns out this excess term defines the electromagnetic interactions between charged particles mediated by the gauge field.

Thus, an invariant Lagrangian for QED can be written in the following form,

$$\begin{aligned} \mathcal{L}_{QED} =& \mathcal{L}_{Dirac} + \mathcal{L}_{Maxwell} + \mathcal{L}_{interaction} \\ =& \bar{\psi}(i\gamma^\mu \partial_\mu - m)\psi - \frac{1}{4}F^{\mu\nu}F_{\mu\nu} - q\bar{\psi}\gamma^\mu \psi A_\mu \end{aligned} \tag{2.5}$$

where $F^{\mu\nu} = \partial_\mu A_\nu - \partial_\nu A_\mu$ is the field strength tensor. The equations of motion for the vector field A_μ will now give us the inhomogeneous Maxwell equations.

$$\partial_\mu F^{\mu\nu} = q J^\nu_{em} \tag{2.6}$$

$J^\nu_{em} = \bar{\psi}\gamma^\nu\psi$ is the electromagnetic current density. The equation of motion of the Dirac field ψ gives the Dirac equation.

$$(i\gamma^\mu D_\mu - m)\psi = 0 \tag{2.7}$$

2.2 The Electroweak Theory

Electromagnetic and weak forces are combined by S. L. Glashow [17], and the Higgs mechanism [18] is incorporated into the theory by Weinberg[19] and Salam [20] to generate the masses of the fermions and the gauge bosons.

The electroweak theory is a chiral theory, meaning that the theory distinguishes the left- and right-handed particles. Left-handed particles form $SU(2)$ doublets, but right-handed particles do not carry a weak charge; thus, they are $SU(2)$ singlets.

Left-handed doublets:

$$Q^i = \begin{pmatrix} u \\ d \end{pmatrix}_L, \begin{pmatrix} c \\ s \end{pmatrix}_L, \begin{pmatrix} t \\ b \end{pmatrix}_L ; \quad L^i = \begin{pmatrix} \nu_e \\ e \end{pmatrix}_L, \begin{pmatrix} \nu_\mu \\ \mu \end{pmatrix}_L, \begin{pmatrix} \nu_\tau \\ \tau \end{pmatrix}_L \tag{2.8}$$

Right-handed singlets:

$$e^i = e_R, \mu_R, \tau_R; \quad u^i = u_R, c_R, t_R; \quad d^i = d_R, s_R, b_R \tag{2.9}$$

For simplicity, the subscript i is removed for the rest of the thesis.

Any Dirac field can be written as a combination of left- and right-handed states,

$$\psi = \psi_L + \psi_R = \Big(\frac{1-\gamma^5}{2}\Big)\psi + \Big(\frac{1+\gamma^5}{2}\Big)\psi. \tag{2.10}$$

Fields transform under $SU(2)$ gauge group with isospin operator $\mathbf{t}$,

$$\begin{aligned} \psi_L \rightarrow \psi_L^{'} &= e^{-i\mathbf{t}\cdot\boldsymbol{\alpha}(x)}\psi_L = e^{-\frac{i}{2}\boldsymbol{\sigma}\cdot\boldsymbol{\alpha}(x)}\psi_L, \\ \psi_R \rightarrow \psi_R^{'} &= e^{-i\mathbf{t}\cdot\boldsymbol{\alpha}(x)}\psi_R = \psi_R \end{aligned} \tag{2.11}$$

where $\boldsymbol{\sigma}$ is the pauli matrices and $\mathbf{t}$ is 0 for singlets and $\boldsymbol{\sigma}/2$ for doublets. The gauge field of the SU(2) group is $\mathbf{W}_\mu(x) = (W^1_\mu(x), W^2_\mu(x), W^3_\mu(x))$ and the covariant derivative is

$$D_\mu = \partial_\mu - ig\mathbf{t}.\mathbf{W}_\mu \tag{2.12}$$

where g is the coupling constant, the gauge field transformed accordingly,

$$\mathbf{t}\cdot\mathbf{W}_\mu \to \mathbf{t}\cdot\mathbf{W}_\mu + \frac{1}{g}\boldsymbol{\sigma}\cdot(\partial_\mu\boldsymbol{\alpha}) - \mathbf{t}\cdot(\boldsymbol{\alpha}\times\mathbf{W}_\mu). \tag{2.13}$$

The problem here is that all three of the $SU(2)_L$ gauge bosons only interact with left-handed fermions. However, it is experimentally established that the neutral current interacts with both left- and right-handed particles. The problem is solved by mixing this interaction with another symmetry that couples to both chiral fermions. The g' is the coupling constant of B_μ field.

$$D_\mu = \partial_\mu - ig'YB_\mu\,, \tag{2.14}$$

$$\psi \to e^{iY\beta(x)}\psi\,, \tag{2.15}$$

$$B_\mu \to B_\mu + \frac{1}{g'}\partial_\mu\beta\,. \tag{2.16}$$

The charge of B_μ field is called the weak hypercharge, denoted with Y, and it is determined by Nishijima-Gell-Mann's law:

$$Q = I^3 + Y. \tag{2.17}$$

Q is the electric charge and I^3 is the third component of the isospin. Fermion quantum numbers are listed in Table 2.2.

Table 2.2: The quantum number assignments of the fermions in the SM.

	I^3	Y	Q		I^3	Y	Q
u_L	$\frac{1}{2}$	$\frac{1}{6}$	$\frac{2}{3}$	u_R	0	$\frac{2}{3}$	$\frac{2}{3}$
d_L	$-\frac{1}{2}$	$\frac{1}{6}$	$-\frac{1}{3}$	d_R	0	$-\frac{1}{3}$	$-\frac{1}{3}$
e_L	$-\frac{1}{2}$	$-\frac{1}{2}$	-1	e_R	0	-1	-1
ν_L	$\frac{1}{2}$	$-\frac{1}{2}$	0				

B_μ field interacts with all fermions but $\mathbf{W}_\mu$ field only interacts with left handed fermions. Interaction terms in the Lagrangian are in the below form,

$$\begin{aligned}\bar{\psi_L} i\gamma^\mu D_{\mu L}\psi_L &= \bar{\psi_L} i\gamma^\mu(\partial_\mu - ig\mathbf{t}.\mathbf{W}_\mu - ig'YB_\mu)\psi_L \\ &= \bar{\psi_L} i\gamma^\mu(\partial_\mu - \frac{ig}{2}(\sigma_1 W_\mu^1 + \sigma_2 W_\mu^2 + \sigma_3 W_\mu^3) - ig'YB_\mu)\psi_L, \quad (2.18)\\ \bar{\psi_R} i\gamma^\mu D_{\mu R}\psi_R &= \bar{\psi_R} i\gamma^\mu(\partial_\mu - ig'YB_\mu)\psi_R.\end{aligned}$$

Looking closer at the above equations, one will notice that W_μ^3 and B_μ fields act on the same fermions. Since neutrinos have no electric charge, they do not interact with the photon field A_μ, a known fact from QED. Therefore, if we look at electron and neutrino interactions with gauge fields

$$\frac{1}{2}\Big[\bar{\nu_{eL}}\gamma^\mu\nu_{eL}(gW_\mu^3 - g'B_\mu) - \bar{e_L}\gamma^\mu e_L(gW_\mu^3 + g'B_\mu) - 2\bar{e_R}\gamma^\mu e_R g'B_\mu\Big], \quad (2.19)$$

it can be seen that W_μ^3 mix with B_μ field and become the neutral weak boson $Z_\mu \propto (gW_\mu^3 - g'B_\mu)$ and the photon $A_\mu \propto (gW_\mu^3 + g'B_\mu)$. This mixing can be expressed as a rotation.

$$\begin{pmatrix} Z_\mu \\ A_\mu \end{pmatrix} = \begin{pmatrix} \cos\theta_W & -\sin\theta_W \\ \sin\theta_W & \cos\theta_W \end{pmatrix} \begin{pmatrix} W_\mu^3 \\ B_\mu \end{pmatrix} \quad (2.20)$$

where θ_W is the Weinberg angle or weak mixing angle. This angle is defined as a relation between the coupling constants,

$$\cos\theta_W = \frac{g}{\sqrt{g^2 + g'^2}}, \quad \sin\theta_W = \frac{g'}{\sqrt{g^2 + g'^2}} \quad (2.21)$$

and the other two components of $\mathbf{W}_\mu$ mix to give

$$W_\mu^\pm = \frac{1}{\sqrt{2}}(W^1 \mp iW_\mu^2). \quad (2.22)$$

However, there is a problem. Introducing a mass term to the gauge bosons will break the gauge invariance of the Lagrangian, but it is known experimentally that $W_\mu^\pm$ and Z_μ bosons are massive. Therefore, there must be another mechanism that gives mass to the weak gauge bosons.

2.3 Spontaneous Symmetry Breaking

An illustrative example of getting familiar with SSB is considering a real scalar field with the Lagrangian below:

$$\mathcal{L} = \frac{1}{2}(\partial_\mu \phi)^2 - V(\phi). \tag{2.23}$$

This is a familiar ϕ^4 theory where the potential is

$$V(\phi) = +\frac{1}{2}m^2\phi^2 + \frac{\lambda}{4!}\phi^4 \tag{2.24}$$

and the ground state is located at $\phi_0 = 0$ if m^2 is positive. An interesting case arises when $m^2 \to -\mu^2$.

$$V(\phi) = -\frac{1}{2}\mu^2\phi^2 + \frac{\lambda}{4!}\phi^4 \tag{2.25}$$

Now, the solution has two minima at

$$\phi_0 = \pm v = \pm\mu\sqrt{\frac{6}{\lambda}}. \tag{2.26}$$

In the beginning, the Lagrangian 2.23 with potential 2.24 has the discrete symmetry $\phi \to -\phi$. Now, when the potential is in the form 2.25, the system will choose one of the minima. A small perturbation from that minima

$$\phi(x) = v + \xi(x) \tag{2.27}$$

will result in the below Lagrangian

$$\mathcal{L} = \frac{1}{2}(\partial_\mu \xi)^2 - \frac{1}{2}(2\mu^2)\xi^2 - \sqrt{\frac{\lambda}{6}}\mu\xi^3 - \frac{\lambda}{4!}\xi^4 \tag{2.28}$$

and it is apparent that the symmetry of the ground state $\phi_0 \to -\phi_0$ is broken. From that Lagrangian, we can read the field ξ has mass $\sqrt{2}\mu$.

2.3.1 The Higgs Mechanism

Higgs field is introduced as a $SU(2)_L$ doublet with 4 real components

$$\phi = \begin{pmatrix} \phi^+ \\ \phi^0 \end{pmatrix} = \frac{1}{\sqrt{2}} \begin{pmatrix} \phi_3 + i\phi_4 \\ \phi_1 + i\phi_2 \end{pmatrix} \tag{2.29}$$

where

$$\phi^\dagger\phi = (\phi^+)^*\phi^+ + (\phi^0)^*\phi^0 = \frac{1}{2}(\phi_1^2 + \phi_2^2 + \phi_3^2 + \phi_4^2) = \frac{v^2}{2} \tag{2.30}$$

Unlike in Section 2.3 here, there are infinitely many different ways to choose the field values, resulting in an infinitely degenerate vacuum. A configuration that works best can be freely chosen. Hence, three of the fields in their vacuum configurations can be set to zero $(\phi_2)_0 = (\phi_3)_0 = (\phi_4)_0 = 0$ and $(\phi_1)_0 = v$ can be chosen. This selection of the vacuum also ensures the conservation of charge.

Any excitation around the vacuum can now be written as

$$\phi = \frac{1}{\sqrt{2}} \begin{pmatrix} (\xi_2 + i\xi_1)/2 \\ v + h - i\xi_3/2 \end{pmatrix} \tag{2.31}$$

when $v \gg |h|, |\boldsymbol{\xi}|$ the equation can rewritten as

$$\phi = e^{i\frac{\boldsymbol{\xi}}{v}\cdot\frac{\boldsymbol{\sigma}}{2}} \begin{pmatrix} 0 \\ \frac{v+h}{\sqrt{2}} \end{pmatrix}. \tag{2.32}$$

Now, it can be realized that the above equation defines a gauge transformation, and the three fields $\boldsymbol{\xi}$ have disappeared if the following transformation is applied

$$\phi \to \phi' = e^{-i\frac{\boldsymbol{\xi}}{v}\cdot\frac{\boldsymbol{\sigma}}{2}}\phi \tag{2.33}$$

and the gauge field $\boldsymbol{W}_\mu$ also transform as

$$\boldsymbol{W}'_\mu \cdot \boldsymbol{t} = \boldsymbol{W}_\mu - \frac{1}{gv}\partial_\mu \boldsymbol{\xi} \cdot \mathbf{t}. \tag{2.34}$$

The field $\boldsymbol{\xi}$ reappears in the gauge field as a longitudinal component. These three fields are known as Goldstone bosons. They are generated by the Higgs doublet, but they are absorbed into the longitudinal components of three massive gauge bosons.

The Higgs field contribution to the SM Lagrangian is written as follows:

$$\mathcal{L} = |D_\mu\phi|^2 + \mu^2\phi^\dagger\phi - \lambda(\phi^\dagger\phi)^2. \tag{2.35}$$

If the steps outlined in Section 2.3 are followed for the Higgs doublet, the mass of the Higgs field can be calculated as $m_h = \mu\sqrt{2} = v\sqrt{2\lambda}$.

2.3.2 The Gauge Boson Masses

The mass of the gauge bosons comes from the covariant derivative that acts on the Higgs field, i.e., the kinetic term for the Higgs field. The Higgs field has isospin 1/2 and hypercharge 1/2. The covariant derivative acts on the Higgs field, as shown below:

$$\begin{aligned} D_\mu\phi &= (\partial_\mu - ig\mathbf{t}.\mathbf{W}_\mu - ig'YB_\mu)\phi \\ &= \frac{1}{\sqrt{2}}\begin{pmatrix} \partial_\mu - i\frac{g}{2}W_\mu^3 - i\frac{g'}{2}B_\mu & -i\frac{g}{2}(W_\mu^1 - iW_\mu^2) \\ -i\frac{g}{2}(W_\mu^1 + iW_\mu^2) & \partial_\mu + i\frac{g}{2}W_\mu^3 - i\frac{g'}{2}B_\mu \end{pmatrix}\begin{pmatrix} 0 \\ v + h(x) \end{pmatrix} \\ &= \frac{1}{\sqrt{2}}\begin{pmatrix} -\frac{ig}{\sqrt{2}}W_\mu^+(v + h(x)) \\ \partial_\mu h + i(v + h)(\frac{g}{2}W_\mu^3 - \frac{g'}{2}B_\mu) \end{pmatrix}. \end{aligned} \tag{2.36}$$

Mass terms arise from products such as W^+W^-. These terms can be seen in the Lagrangian given in equation 2.35.

$$(D_\mu\phi)^\dagger(D^\mu\phi) \supset \frac{1}{4}g^2W^{\mu-}W_\mu^+(v+h)^2 + \frac{1}{2}\partial^\mu h\partial_\mu h + \frac{1}{8}(v+h)^2(gW_\mu^3 - g'B_\mu)^2 \tag{2.37}$$

Therefore, the Lagrangian consisting of the mass terms of the gauge bosons will be written as

$$\mathcal{L}_{\text{mass}} = \frac{1}{4}(gv)^2W^{\mu-}W_\mu^+ + \frac{1}{8}v^2\begin{pmatrix} W^{\mu 3} & B^\mu \end{pmatrix}\begin{pmatrix} g^2 & -gg' \\ -gg' & g'^2 \end{pmatrix}\begin{pmatrix} W_\mu^3 \\ B_\mu \end{pmatrix}. \tag{2.38}$$

It is seen that the mass of the charged bosons is $m_{W^\pm} = \frac{1}{2}gv$. However, the second term contains off-diagonal elements. To obtain the physical bosons, the mass matrix must be diagonalized. The 2×2 matrix has eigenvalues $\lambda_1 = 0$ and $\lambda_2 = (g^2 + g'^2)$, which yields the following mass matrix for the neutral bosons:

$$\mathcal{L}_{\text{neutral bosons}} = \frac{1}{2}\begin{pmatrix} A^\mu & Z^\mu \end{pmatrix}\begin{pmatrix} 0 & 0 \\ 0 & \frac{v^2}{4}(g^2 + g'^2) \end{pmatrix}\begin{pmatrix} A_\mu \\ Z_\mu \end{pmatrix}. \tag{2.39}$$

This transformation is the transformation carried out in Section 2.2 to obtain the physical bosons, where a rotation involving the Weinberg angle was applied. After this transformation, the mass matrix will take a diagonal form and the mass of the photon and the Z boson can be determined as $m_A = 0$ and $m_Z = \frac{1}{2}v\sqrt{g^2 + g'^2}$.

2.3.3 Fermion masses

Every fermion can be written in left- and right-handed components as in equation 2.10. Given the Dirac Lagrangian, the fields are projected into left- and right-handed components

$$\begin{aligned}\mathcal{L} =&\bar{\psi}_L i\gamma^\mu \partial_\mu \psi_L + \bar{\psi}_R i\gamma^\mu \partial_\mu \psi_R + \bar{\psi}_L i\gamma^\mu \partial_\mu \psi_R + \bar{\psi}_R i\gamma^\mu \partial_\mu \psi_L \\ &- \bar{\psi}_L m\psi_L - \bar{\psi}_R m\psi_R - \bar{\psi}_L m\psi_R - \bar{\psi}_R m\psi_L.\end{aligned} \tag{2.40}$$

By applying $(1-\gamma^5)(1+\gamma^5) = 0$ and $\{\gamma^5, \gamma^\mu\} = 0$ to the Lagrangian, several terms will be canceled.

$$\mathcal{L} = i\bar{\psi}_L \gamma^\mu \partial_\mu \psi_L + i\bar{\psi}_R \gamma^\mu \partial_\mu \psi_R - m(\bar{\psi}_L \psi_R + \bar{\psi}_R \psi_L) \tag{2.41}$$

Now it is clear that to obtain the mass, terms of the form $\bar{\psi}_L \psi_R$ and $\bar{\psi}_R \psi_L$ should be sought. These terms arise from the interactions of fermions with the Higgs field, known as the Yukawa terms. In the most general form these interactions are in the form below:

$$\mathcal{L}_{\text{yukawa}} = -Y(\bar{\psi}_L \phi \psi_R + \bar{\psi}_R \tilde{\phi} \psi_L). \tag{2.42}$$

For further details of this sector as well as the other sectors covered in this chapter, the following sources may be consulted: [21] [22] [23] .

CHAPTER 3

THE THEORETICAL FRAMEWORK

Discovery of the Higgs particle is one of the greatest successes of the SM. Having one Higgs doublet is a minimal theory, but theoretically, there are no upper bounds in the number of doublets we can add to the theory. Introducing new doublets can explain some of the enigmatic phenomena in the SM.

In this thesis, we expand the scalar and the gauge sectors of the SM by adding an extra Higgs doublet and an abelian $U(1)_{\mathrm{D}}$ group, respectively. Furthermore, to ensure the theory is anomaly-free, the introduction of right-handed neutrinos is necessary. The Lagrangian of the model is

$$\mathcal{L} = \mathcal{L}_{\mathrm{fermion}} + \mathcal{L}_{\mathrm{scalar}} + \mathcal{L}_{\mathrm{gauge}} + \mathcal{L}_{\mathrm{yukawa}} - V_{\mathrm{scalar}} \tag{3.1}$$

and each term will be explained further. The construction of the theory begins with the inclusion of the scalar doublet in Section 3.1, followed by the introduction of the new boson in Section 3.2. Subsequently, in Section 3.2.3, we perform calculations to determine the couplings of the new boson to SM fermions, which are going to be essential for our further analysis of the ATOMKI anomaly.

From this chapter on, the fermion fields are denoted by capital letters: Q and L for quark and lepton doublets, and U, D, E, and N for right-handed up, down, electron, and neutrino singlets, respectively. The lowercase letters denote their dark charges under the gauge group $U(1)_D$.

3.1 The Two Higgs Doublet Model

The first constraint to the model comes from the ρ parameter [1] [12].

$$\rho = \frac{\sum_{i=1}^{n}[I_i(I_i+1) - Y_i^2]v_i}{\sum_{i=1}^{n} 2Y_i^2 v_i} \tag{3.2}$$

I_i, Y_i and v_i are weak isospin, weak hypercharge and vev of the neutral components of n scalar multiples, respectively. Experimentally the parameter $\rho = \frac{m_W^2}{m_z^2 cos^2\theta_W}$ is observed to be close to unity [24], imposing a crucial constraint on the models construction.

The specific model under consideration is type-I 2HDM, where fermions only couple to one of the Higgs doublet (ϕ_2). Both doublet have hypercharge $Y = 1/2$ and their $U(1)_D$ charges are h_1 and h_2 respectively. The CP-conserving neutral doublets are:

$$\langle\phi_1\rangle = \frac{1}{\sqrt{2}}\begin{pmatrix}0\\ v_1\end{pmatrix}, \quad \langle\phi_2\rangle = \frac{1}{\sqrt{2}}\begin{pmatrix}0\\ v_2\end{pmatrix} \tag{3.3}$$

where $v^2 = v_1^2 + v_2^2 = (246\ GeV)^2$. Following the SSB, three of the fields are absorbed by the $W^{\pm}$ and Z^0 bosons. The remaining five of the eight fields become physical Higgs fields, consisting of a charged Higgs pair, two neutral scalars, and one pseudoscalar.

The general form of the potential in the 2HDM models, being gauge invariant and renormalizable can be written as below [1]:

$$\begin{aligned} V(\phi_1,\phi_2) = {} & m_{11}^2\phi_1^\dagger\phi_1 + m_{22}^2\phi_2^\dagger\phi_2 - (m_{12}^2\phi_1^\dagger\phi_2 + h.c.) + \frac{\lambda_1}{2}(\phi_1^\dagger\phi_1)^2 \\ & + \frac{\lambda_2}{2}(\phi_2^\dagger\phi_2)^2 + \lambda_3(\phi_1^\dagger\phi_1)(\phi_2^\dagger\phi_2) + \lambda_4(\phi_1^\dagger\phi_2)(\phi_2^\dagger\phi_1) \\ & + \left[\frac{\lambda_5}{2}(\phi_1^\dagger\phi_2)^2 + \lambda_6(\phi_1^\dagger\phi_1)\phi_1^\dagger\phi_2 + \lambda_7(\phi_2^\dagger\phi_2)(\phi_1^\dagger\phi_2) + h.c.\right]. \end{aligned} \tag{3.4}$$

2HDMs, in general, suffer from flavour-changing neutral currents (FCNC)[25] at three level. To overcome this problem, one can introduce a Z_2 discrete symmetry, known as the natural flavour conservation (NFC) criterion, as suggested by Glashow and Weinberg [26]. This symmetry ensures each fermion field interacts with only one Higgs doublet, thereby eliminating the FCNCs.

Table 3.1: Z_2 Parities of particles in each 2HDM type [1].

Model	ϕ_1	ϕ_2	U	D	E	Q,L
Type I	-	+	+	+	+	+
Type II	-	+	+	-	-	+
Lepton-specific	-	+	+	+	-	+
Flipped	-	+	+	-	+	+

Different 2HDMs can be defined by Z_2 charges, as shown in Table 3.1. All possible Z_2 charge assignments that eliminate FCNCs are listed here. In each model, fermions couple to the Higgs field with the same Z_2 charge. In type I model, SM fermions couple exclusively to ϕ_2 only.

The Type-I model is realized through the following symmetry,

$$\phi_1 \to -\phi_1, \quad \phi_2 \to \phi_2\,, \tag{3.5}$$

which requires $m_{12} = \lambda_6 = \lambda_7 = 0$. If $m_{12} \neq 0$ then Z_2-symmetry is softly broken. Thus, the potential is now in the form below:

$$\begin{aligned} V(\phi_1,\phi_2) = {} & m_{11}^2\phi_1^\dagger\phi_1 + m_{22}^2\phi_2^\dagger\phi_2 - m_{12}^2(\phi_1^\dagger\phi_2 + \phi_2^\dagger\phi_1) + \frac{\lambda_1}{2}(\phi_1^\dagger\phi_1)^2 \\ & + \frac{\lambda_2}{2}(\phi_2^\dagger\phi_2)^2 + \lambda_3(\phi_1^\dagger\phi_1)(\phi_2^\dagger\phi_2) + \lambda_4(\phi_1^\dagger\phi_2)(\phi_2^\dagger\phi_1) \\ & + \frac{\lambda_5}{2}\left[(\phi_1^\dagger\phi_2)^2 + (\phi_2^\dagger\phi_1)^2\right]. \end{aligned} \tag{3.6}$$

However, this symmetry can be replaced by introducing a new $U(1)$ symmetry [27]. $U(1)_{\rm D}$ symmetry forbids the terms $\phi_1^\dagger\phi_2$ or square of this term if $h_1 \neq h_2$. Thus $m_{12}^2 = 0$ and $\lambda_5 = 0$. If a singlet scalar ϕ_s is introduced, and as will be shown in Section 3.2.1, the dark charge of the singlet is $h_s = h_1 - h_2$. In this case, the term $\phi_1^\dagger\phi_2\phi_s$ is gauge invariant, leading to additional terms in the potential:

$$\begin{aligned} V(\phi_s,\phi_1,\phi_2) = {} & m_\phi^2 + \phi_s^\dagger\phi_s + \frac{\lambda_s}{2}(\phi_s^\dagger\phi_s)^2 + (\mu\phi_1^\dagger\phi_2\phi_s + h.c.) \\ & + \mu_1\phi_1^\dagger\phi_1\phi_s^\dagger\phi_s + \mu_2\phi_2^\dagger\phi_2\phi_s^\dagger\phi_s. \end{aligned} \tag{3.7}$$

Upon a closer inspection, the μ term resembles the m_{12}^2 term when the singlet develops a vev. Thus, the origin of the Z_2 symmetry has been identified. Additionally,

when there is an exact Z_2 symmetry and $\lambda_5 = 0$ in usual 2HDMs an additional Peccei-Quinn symmetry emerges [28]. The spontaneous breaking of the $U(1)_{\mathrm{D}}$ symmetry by the singlet scalar does not result in massless axions, which are associated with Peccei-Quinn symmetry [29].

Now, the scalar part of the Lagrangian can be written with two doublets and a singlet as shown below:

$$\mathcal{L}_{\mathrm{scalar}} = (D_\mu\phi_1)^\dagger(D_\mu\phi_1) + (D_\mu\phi_2)^\dagger(D_\mu\phi_2) + (D_\mu\phi_s)^\dagger(D_\mu\phi_s) \tag{3.8}$$

where the covariant derivative is,

$$\mathcal{D}_\mu = \partial_\mu - igt^aW_\mu^a - ig'YB_\mu - ig_Dq_DX_\mu. \tag{3.9}$$

$t^a = \frac{1}{2}\sigma^a$, σ is the Pauli matrices, hypercharges are given in Table 2.2 and the dark charges will be calculated in Subsection 3.2.1.

$$\mathcal{D}_\mu\langle\phi_i\rangle = \begin{pmatrix} \partial_\mu - \frac{ig}{2}W_\mu^3 - ig'Y_iB_\mu - ig_Dq_{Di}X_\mu & \frac{-ig}{2}(W_\mu^1 - iW_\mu^2) \\ \frac{-ig}{2}(W_\mu^1 + iW_\mu^2) & \partial_\mu + \frac{ig}{2}W_\mu^3 - ig'Y_iB_\mu - ig_Dq_{Di}X_\mu \end{pmatrix} \begin{pmatrix} 0 \\ v_i \end{pmatrix} \tag{3.10}$$

where $i = 1, 2$. If the Higgs singlet only couples to right-handed neutrinos with vev v_s, the covariant derivative will transform as follows:

$$\mathcal{D}_\mu\langle\phi_s\rangle = (\partial_\mu - ig_Dh_sX_\mu)v_s. \tag{3.11}$$

As discussed in Section 2.3.3, writing a mass term requires both left- and right-handed projections of a particle. Since there are no right-handed neutrinos in the SM, a mass term for neutrinos cannot be formulated. The addition of right-handed neutrinos enables the formulation of a Dirac mass term for neutrinos. Thereby, a new term is added to the Yukawa Lagrangian. The singlet scalar also contributes to explaining neutrino masses and introduces an additional term to the Yukawa Lagrangian. The effect of these additional terms on our model is discussed in Section 3.2.1.

Apart from explaining the origin of the Z_2 symmetry, this singlet can also provide an explanation for the smallness of neutrino masses via the seesaw mechanism [30],[31],

[32]. Neutrino masses in the type-I 2HDM model are discussed in this article [1]. There may be different explanations for neutrino masses, but only the vev of the singlet is relevant to our work. Consequently, further discussion of neutrino masses is irrelevant to our study and will not be addressed.

3.2 Extending the 2HDM with $U(1)_D$ symmetry

The new field X_μ corresponding to $U(1)_{\rm D}$ symmetry is allowed to mix with SM B_μ field. $U(1)_{\rm Y}$ and $U(1)_{\rm D}$ symmetries can form a renormalizable kinetic mixing term between them. When the mixing parameter is taken as $\sin\epsilon$, and it is small, the related part of the Lagrangian is given below.

$$\mathcal{L}_{\rm gauge} = -\frac{1}{4}B_{\mu\nu}B^{\mu\nu} - \frac{1}{4}X_{\mu\nu}X^{\mu\nu} - \frac{1}{2}\sin\epsilon X_{\mu\nu}B^{\mu\nu} \tag{3.12}$$

Here $B_{\mu\nu} = \partial_\mu B_\nu - \partial_\nu B_\mu$ and $X_{\mu\nu} = \partial_\mu X_\nu - \partial_\nu X_\mu$ are the field-strength tensors. Before proceeding further, it is essential to determine the potential new dark charges of the particles. These new fields must satisfy the anomaly-free conditions, imposing constraints on possible charge assignments. These constraints will be calculated in the following Section 3.2.1, then the gauge mixing situation will be addressed in Section 3.2.2 and the mass of Z and A' bosons will be calculated. In Section 3.2.3, couplings of the bosons to the SM fermions will be calculated.

3.2.1 $U(1)_D$ charge assignment of 2HDM fields

The SM is an anomaly-free theory. Consequently, when extending our model, it is important to ensure that the new extension is also anomaly-free. The anomaly occurs when the currents of the SM are not conserved, which is also referred to as current non-conservation. The conservation of currents implies that $\langle\partial_\mu J^\mu\rangle = 0$ for any SM forces. However, this conservation equation may not hold in general for triangle diagrams. Specifically, the couplings described below lead to anomalies:

1. $U(1) \times U(1) \times U(1)$
2. $SU(3) \times SU(3) \times U(1)$

3. $SU(2) \times SU(2) \times U(1)$

4. $U(1) - \text{gravity}^2$

Although the equations do not initially vanish, they will be shown to disappear when the SM charges are assigned to them, thus confirming that the SM is anomaly-free. Upon closer examination, it will be noted that each of these couplings involves at least one $U(1)$ field. Therefore, when an additional $U(1)$ field is introduced into the SM, conditions must be imposed to ensure that the new model remains anomaly-free. To understand this better, the process by which anomalies are cancelled in the SM will first be examined, focusing on the first generation of fermions for simplicity.

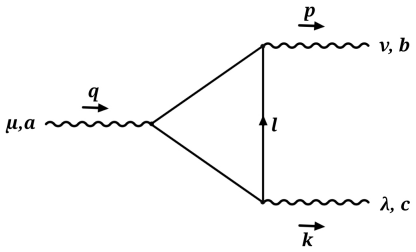

Figure 3.1: A generic triangle diagram. Three legs are representing any SM gauge fields.

For a non-Abelian theory the current can be written as follows:

$$j^{\mu a} = \bar{\psi}\gamma^{\mu}\frac{1-\gamma^5}{2}T^a\psi. \tag{3.13}$$

Here T's are the group generators.γ^5 term leads to the relation,

$$\langle p,\nu,b;k,\lambda,c|\partial_\mu j^{\mu a}|0\rangle = \frac{g^2}{8\pi^2}\epsilon^{\alpha\nu\beta\lambda}p_\alpha k_\beta \cdot Tr[T^a\{T^b,T^c\}]. \tag{3.14}$$

Therefore, unless the trace in the equation vanishes, the current is not conserved. Left-handed doublets L and Q are assigned hypercharges of $-1/2$ and $1/6$ respectively, and right-handed singlets E, U, D are given hypercharges of $-1, 2/3$ and, $-1/3$ respectively. The calculations for each of these cases for the SM are detailed below.

1. $U(1)_Y^3$:

The non-abelian scenario can be generalized here where the group generator is the hypercharge $Tr[T^a] = Tr[Y] = Y$.

$$\langle \partial_\mu j^\mu \rangle \propto Tr[Y^3] = \sum_f (Y_L^3 - Y_R^3) \tag{3.15}$$

Left and right-handed particles contribute with an opposite sign. The summation now becomes;

$$2(-1)^3 + 2 \times 3 \left(\frac{1}{3}\right)^3 - \left((-2)^3 + 3\left(\frac{4}{3}\right)^3 + 3\left(-\frac{2}{3}\right)^3\right) \tag{3.16}$$

which equals zero. Taking into account that two particles are in doublets, and each quark has three colour states and inserting the weak hypercharge values of each of these fields (listed in Table 2.2) results in a vanishing combination. Summing over all these states yields the coefficients that appear before the parentheses.

2. $SU(3)^2 \times U(1)_Y$:

$$\langle \partial_\mu j^\mu \rangle \propto Tr[Y\{\tau^b, \tau^c\}] \tag{3.17}$$

$$= \sum_f (Y_L - Y_R) Tr[\{\tau^b, \tau^c\}] \tag{3.18}$$

Here, the equation can vanish if either the first or the second term is zero. Consider the first term and remember this interaction only affects quarks.Thus,

$$2 \times 3\left(\frac{1}{6}\right) - \left(3 \times \frac{2}{3} + 3 \times \left(-\frac{1}{3}\right)\right) = 0 \tag{3.19}$$

3. $SU(2)^2 \times U(1)_Y$:

Calculations are similar here;

$$\langle \partial_\mu j^\mu \rangle \propto Tr[Y\{t^b, t^c\}] = \frac{1}{2} Tr[Y]\delta^{bc} \tag{3.20}$$

This time, only left-handed particles contribute to this interaction

$$\sum Y_L = 2 \times \left(-\frac{1}{2}\right) + 2 \times 3\left(\frac{1}{6}\right) = 0 \tag{3.21}$$

4. $U(1)_Y \times$gravity^2:

Lastly, this anomaly has to be cancelled. It appears to have a similar structure to the previous couplings. Since gravity couples to all fermions, one final equation is obtained,

$$\sum_f (Y_L - Y_R) = 2\times(-1) + 2\times 3\left(\frac{1}{3}\right) - \left(-2 + 3\left(\frac{4}{3}\right) + 3\left(-\frac{2}{3}\right)\right) \quad (3.22)$$

and it is also seen that this last equation equals zero.

In case of $U(1)_D$ extension, the following anomaly equations will be obtained:

1. $SU(3) \times SU(3) \times U(1)_D$
2. $SU(2) \times SU(2) \times U(1)_D$
3. $U(1) \times U(1) \times U(1)_D$
4. $U(1) \times U(1)_D \times U(1)_D$
5. $U(1)_D \times U(1)_D \times U(1)_D$
6. $U(1)_D$-gravity^2

Where doublets L and Q have the new dark charges l and q respectively and singlets E, N, U, D have dark charges e, ν, u and d respectively, similar calculations are carried to get the below equations:

$$\begin{aligned}
&2q - u - d = 0 \\
&l + 3q = 0 \\
&3l + q - 6e - 8u - 2d = 0 \\
&q^2 - l^2 + e^2 - 2u^2 + d^2 = 0 \\
&2l^3 + 6q^3 - e^3 - \nu^3 - 3e^3 - 3d^3 = 0 \\
&2l + 6q - e - \nu - 3u - 3d = 0
\end{aligned} \quad (3.23)$$

However, those are not the only constraints. The extended Lagrangian should be gauge invariant under $U(1)_D$ symmetry. Other constraints are coming from this invariance. If the fields are transformed as follows,

$$
\begin{aligned}
L &\to L' = \exp[il\alpha(x)]L, \\
Q &\to Q' = \exp[iq\alpha(x)]Q, \\
E &\to E' = \exp[ie\alpha(x)]E, \\
U &\to U' = \exp[iu\alpha(x)]U, \\
D &\to D' = \exp[id\alpha(x)]D, \\
\phi_1 &\to \phi_1' = \exp[ih_1\alpha(x)]\phi_1, \\
\phi_2 &\to \phi_2' = \exp[ih_2\alpha(x)]\phi_2, \\
\phi_s &\to \phi_s' = \exp[ih_s\alpha(x)]\phi_s.
\end{aligned}
\tag{3.24}
$$

The SM Yukawa Lagrangian,

$$
\mathcal{L}_{SM}^{Yukawa} = y_2^u \bar{Q}\tilde{\phi}_2 U + y_2^D \bar{Q}\phi_2 D + y_2^e \bar{L}\phi_2 E + h.c. \tag{3.25}
$$

along with the newly added right-handed neutrino component,

$$
\mathcal{L}_N^{Yukawa} = y_s^l \bar{L}\tilde{\phi}_2 N + y_s^\nu \bar{N}\phi_s N \tag{3.26}
$$

will be gauge invariant if the following conditions are satisfied:

$$
\begin{aligned}
\nu - l - \phi_2 &= 0, \\
2\nu + \phi_s &= 0.
\end{aligned}
\tag{3.27}
$$

One last condition comes from the scalar potential,

$$
V_s = m_s^2 \phi_s^\dagger \phi_s + \frac{\lambda_s}{2}(\phi_s^\dagger \phi_s)^2 + \mu_1 \phi_1^\dagger \phi_1 \phi_s^\dagger \phi_s + \mu_2 \phi_2^\dagger \phi_2 \phi_s^\dagger \phi_s + (\mu \phi_1^\dagger \phi_2 \phi_s + h.c.) \tag{3.28}
$$

The invariance of this part yields:

$$
-\phi_1 + \phi_2 + \phi_s = 0. \tag{3.29}
$$

By solving the anomaly equations, the $U(1)_D$ charges of particles are determined in

Table 3.2: Possible $U(1)_D$ charge assignments of fields [2].

	U	D	Q	L	E	N	ϕ_2	ϕ_1
Model A	$\frac{1}{2}$	$-\frac{1}{2}$	0	0	$-\frac{1}{2}$	$\frac{1}{2}$	$\frac{1}{2}$	$-\frac{1}{2}$
Model B	$-\frac{1}{2}$	$\frac{1}{2}$	0	0	$\frac{1}{2}$	$-\frac{1}{2}$	$-\frac{1}{2}$	$\frac{1}{2}$
Model C	$\frac{1}{4}$	$-\frac{1}{2}$	$-\frac{1}{8}$	$\frac{3}{8}$	0	$\frac{3}{4}$	$\frac{3}{8}$	$-\frac{9}{8}$
Model D	$\frac{1}{2}$	0	$\frac{1}{4}$	$-\frac{3}{4}$	-1	$-\frac{1}{2}$	$\frac{1}{4}$	$\frac{5}{4}$
Model E	0	$\frac{1}{2}$	$\frac{1}{4}$	$-\frac{3}{4}$	$-\frac{1}{2}$	-1	$-\frac{1}{4}$	$\frac{7}{4}$
Model F	$\frac{2}{3}$	$\frac{1}{3}$	$\frac{1}{2}$	$-\frac{3}{2}$	$-\frac{5}{3}$	$-\frac{4}{3}$	$\frac{1}{6}$	$\frac{17}{6}$
Model G	$-\frac{1}{6}$	$\frac{1}{3}$	$\frac{1}{12}$	$-\frac{1}{4}$	0	$-\frac{1}{2}$	$-\frac{1}{4}$	$\frac{3}{4}$
Model B-L	$\frac{1}{6}$	$\frac{1}{6}$	$\frac{1}{6}$	$-\frac{1}{2}$	$-\frac{1}{2}$	$-\frac{1}{2}$	0	1
Minimal B-L	$\frac{1}{6}$	$\frac{1}{6}$	$\frac{1}{6}$	$-\frac{1}{2}$	$-\frac{1}{2}$	$-\frac{1}{2}$	0	-

terms of the charges of the right-handed up and down quarks:

$$\begin{aligned} u &= u, & d &= d, \\ e &= -(2u+d), & \phi_1 &= \frac{1}{2}(5u+7d), \\ \nu &= -(u+2d), & \phi_2 &= \frac{1}{2}(u-d), \\ l &= -\frac{3}{2}(u+d), & \phi_s &= 2(u+2d), \\ q &= \frac{1}{2}(u+d). \end{aligned} \tag{3.30}$$

There are two free parameters; thus, various different scenarios can be found. Some of representative charge assignments are given in Table 3.2.

3.2.2 Diagonalization of Mass Squared Matrix of the Gauge Bosons

To remove the mixing between B_μ & X_μ from eqn 3.12 we apply the following transformation

$$\begin{pmatrix} \tilde{B}_\mu \\ W_{3\mu} \\ \tilde{X}_\mu \end{pmatrix} = \begin{pmatrix} 1 & 0 & \sin\epsilon \\ 0 & 1 & 0 \\ 0 & 0 & \cos\epsilon \end{pmatrix} \begin{pmatrix} B_\mu \\ W_{3\mu} \\ X_\mu \end{pmatrix} \equiv V_1 \begin{pmatrix} B_\mu \\ W_{3\mu} \\ X_\mu \end{pmatrix}. \tag{3.31}$$

After this transformation, the Lagrangian in eqn 3.12 will be free of mixing terms,

$$\mathcal{L}'_{gauge} = -\frac{1}{4}\tilde{B}_{\mu\nu}\tilde{B}^{\mu\nu} - \frac{1}{4}\tilde{X}_{\mu\nu}\tilde{X}^{\mu\nu}. \tag{3.32}$$

Next, we rotate the W_μ and $\tilde{B}$ fields by Weinberg angle θ_W. While this angle diagonalizes the mass matrix in the SM case, the transformation does not result in a diagonal mass matrix due to the modifications made to the SM.

$$\begin{pmatrix} A_\mu \\ \tilde{W}_{3\mu} \\ \tilde{X}_\mu \end{pmatrix} = \begin{pmatrix} \cos\theta_W & \sin\theta_W & 0 \\ -\sin\theta_W & \cos\theta_W & 0 \\ 0 & 0 & 1 \end{pmatrix} \begin{pmatrix} \tilde{B}_\mu \\ W_{3\mu} \\ \tilde{X}_\mu \end{pmatrix} \equiv V_2 \begin{pmatrix} \tilde{B}_\mu \\ W_{3\mu} \\ \tilde{X}_\mu \end{pmatrix} \tag{3.33}$$

Therefore, we apply one last transformation to obtain the diagonal mass matrix:

$$\begin{pmatrix} A_\mu \\ Z_\mu \\ A'_\mu \end{pmatrix} = \begin{pmatrix} 1 & 0 & 0 \\ 0 & \cos\tau & \sin\tau \\ 0 & -\sin\tau & \cos\tau \end{pmatrix} \begin{pmatrix} A_\mu \\ \tilde{W}_{3\mu} \\ \tilde{X}_\mu \end{pmatrix} \equiv V_3 \begin{pmatrix} A_\mu \\ \tilde{W}_{3\mu} \\ \tilde{X}_\mu \end{pmatrix}. \tag{3.34}$$

Considering an abelian vector boson, there is another mechanism, the Stueckelberg mechanism, that can give mass to them without spoiling the gauge invariance and renormalizability [33]. In this mechanism, the abelian vector boson is coupled to an axionic scalar field. The neutral electroweak gauge bosons can gain mass via both the axionic field and the Higgs field in a scenario where the SM is extended by Stueckelberg mechanism[34][35]. There is also a study where a Stueckelberg extension of the 2HDM is discussed [36]. In this thesis, the mass of the $U(1)_{\mathrm{D}}$ boson will be acquired via both Higgs and Stueckelberg mechanisms. The first term of equation 3.35 corresponds to Stueckelberg mass m_S, which will contribute to overall A' and Z boson masses.

$$\frac{1}{2}m_S^2 X_\mu X^\mu + (D_\mu\phi_s)^\dagger(D^\mu\phi_s) + \sum_{i=1}^{2}(D_\mu\phi_i)^\dagger(D^\mu\phi_i) \to \mathcal{L}_{mass} + \cdots \tag{3.35}$$

Recalling equations 3.10 and 3.11, the above part of the Lagrangian will lead to the mass matrix after transforming the initial fields to the physical ones by reversing the transformations given in equations 3.31, 3.33, and 3.34.

$$\begin{pmatrix} B_\mu \\ W_{3\mu} \\ X_\mu \end{pmatrix} = (V_3 V_2 V_1)^{-1} \begin{pmatrix} A_\mu \\ Z_\mu \\ A'_\mu \end{pmatrix} \tag{3.36}$$

$$= \begin{pmatrix} \cos\theta_W & -\cos\tau\sin\theta_W - \sin\tau\tan\epsilon & \sin\theta_W\sin\tau - \cos\tau\tan\epsilon \\ \sin\theta_W & \cos\theta_W\cos\tau & -\cos\theta_W\sin\tau \\ 0 & \sec\epsilon\sin\tau & \cos\tau\sec\epsilon \end{pmatrix} \begin{pmatrix} A_\mu \\ Z_\mu \\ A'_\mu \end{pmatrix} \tag{3.37}$$

Here, a new variable is defined $\tan\beta \equiv v_2/v_1$. When the last transformation satisfies the below relation

$$\tan 2\tau = \frac{a - 2m_{ZSM}\, v\, g_D\, b}{m_{ZSM}^2(b^2-1) + \sec^2\epsilon\left[m_S^2 + g_D^2 v^2(\cos^2\beta\, h_1^2 + \sin^2\beta\, h_2^2) + g_D^2 v_s^2 h_s^2\right] - ab\sin\epsilon}$$

$$a = 2m_{ZSM} v g_D(\cos^2\beta\, h_1 + \sin^2\beta\, h_2)\,, \qquad b = \tan\epsilon\sin\theta_W\,, \tag{3.38}$$

the Lagrangian corresponding to the boson masses will be in the given diagonal form,

$$\mathcal{L}_{\text{mass}} = \frac{1}{2}\begin{pmatrix} A_\mu & Z_\mu & A'_\mu \end{pmatrix} \begin{pmatrix} 0 & 0 & 0 \\ 0 & M_Z^2 & 0 \\ 0 & 0 & M_{A'}^2 \end{pmatrix} \begin{pmatrix} A_\mu \\ Z_\mu \\ A'_\mu \end{pmatrix}. \tag{3.39}$$

Therefore, square of the Z and A' masses are found as shown below respectively:

$$\begin{aligned} M_Z^2 =& m_S^2\sin^2\tau\sec^2\epsilon + g_D^2\sin^2\tau\sec^2\epsilon(v^2(\cos^2\beta h_1^2 + \sin^2\beta h_2^2) + v_s^2 h_s^2) \\ & - 2m_{ZSM} v g_D\sin\tau\sec\epsilon(\cos^2\beta h_1 + \sin^2\beta h_2)(\cos\tau + \sin\theta_W\sin\tau\tan\epsilon) \\ & + m_{ZSM}^2(\cos\tau + \sin\theta_W\sin\tau\tan\epsilon)^2 \end{aligned} \tag{3.40}$$

$$
\begin{aligned}
M_{A'}^2 =& m_S^2 \cos^2\tau \sec^2\epsilon + g_D^2 \cos^2\tau \sec^2\epsilon (v^2(\cos^2\beta h_1^2 + \sin^2\beta h_2^2) + v_s^2 h_s^2) \\
&+ 2 m_{ZSM} v g_D \cos\tau \sec\epsilon (\cos^2\beta h_1 + \sin^2\beta h_2)(\sin\tau - \sin\theta_W \cos\tau \tan\epsilon) \\
&+ m_{ZSM}^2 (\sin\tau - \sin\theta_W \cos\tau \tan\epsilon)^2
\end{aligned}
\tag{3.41}
$$

3.2.3 Calculation of the Relevant Coupling Constants

When the covariant derivative 3.9 acts on the fermionic fields,

$$
\mathcal{L}_{\text{fermion}} = \sum_i \bar{\psi}_i i \not{D} \psi_i \tag{3.42}
$$

we obtain the interaction terms between fermions and bosons. Those interactions between SM fermions with Z and A' bosons have vector and axial parts in general.

$$
\mathcal{L}_{\text{interaction}} = \sum_i \bar{\psi}_i \gamma^\mu (C_i^V + C_i^A \gamma_5) \psi_i Z_\mu + \bar{\psi}_i \gamma^\mu (\varepsilon_i^V + \varepsilon_i^A \gamma_5) \psi_i A'_\mu \tag{3.43}
$$

if we define a new variable here which is related to the third component of the isospin, λ is 1 for u, ν and -1 for d, e. The covariant derivative will act on the fermionic fields. But it will act differently to the left- and right-handed fermions. But for each fermion we can write $\psi = \psi_L + \psi_R$ where $\psi_L = \frac{1-\gamma^5}{2}$ and $\psi_R = \frac{1+\gamma^5}{2}$. Finally, changing the interaction basis to the physical one by applying equation 3.37 will give the result.

$$
\begin{aligned}
&\mathcal{D}\psi^i \supset \\
&\Bigg[(\frac{-i\lambda g}{4}\sin\theta_W - \frac{-ig'}{2}(Y_L^i + Y_R^i)\cos\theta_W \\
&+ \left(\frac{i\lambda g}{4}\sin\theta_W + \frac{ig'}{2}(Y_L^i - Y_R^i)\cos\theta_W\right)\gamma^5\Bigg] A_\mu\psi^i + \\
&\Bigg[\Big(\frac{-i\lambda g}{4}\cos\theta_W\cos\tau + \frac{ig'}{2}(Y_L^i + Y_R^i)(\cos\tau\sin\theta_W + \sin\tau\tan\epsilon) \\
&- \frac{ig_D}{2}(q_L^i + q_R^i)\sec\epsilon\sin\tau\Big) + \Big(\frac{i\lambda g}{4}\cos\theta_W\cos\tau + \\
&\frac{ig'}{2}(Y_R^i - Y_L^i)(\cos\tau\sin\theta_W + \sin\tau\tan\epsilon) + \frac{ig_D}{2}(q_L^i - q_R^i)\sec\epsilon\sin\tau\Big)\gamma^5\Bigg] Z_\mu\psi^i + \\
&\Bigg[\Big(\frac{i\lambda g}{4}\cos\theta_W\sin\tau - \frac{ig'}{2}(Y_L^i + Y_R^i)(\sin\theta_W\sin\tau - \cos\tau\tan\epsilon) - \\
&\frac{ig_D}{2}(q_L^i + q_R^i)\cos\tau\sec\epsilon\Big) + \Big(\frac{-i\lambda g}{4}\cos\theta_W\sin\tau + \\
&\frac{ig'}{2}(Y_L^i - Y_R^i)(\sin\theta_W\sin\tau - \cos\tau\tan\epsilon) + \frac{ig_D}{2}(q_L^i - q_R^i)\cos\tau\sec\epsilon\Big)\gamma^5\Bigg] A'_\mu\psi^i
\end{aligned}
\tag{3.44}
$$

Here Y_L, Y_R and q_L, q_R are the hyper-charges and dark charges of the given left- and right-handed fields respectively. The axial part of A_μ in the covariant derivative vanishes, and the vector part gives the SM electromagnetic current. Using this covariant derivative in equation 3.42, applying the relation $g\sin\theta = g'\cos\theta = e$ and comparing the terms with equation 3.43 will give the coupling strengths. One by one, the coupling of each fermion to Z and A' bosons are calculated and given in Table 3.3 and Table 3.4, respectively. Superscripts V denotes vector, and A denotes axial coupling.

Table 3.3: Vector and axial couplings of fermions to Z boson. Here u and d are the free dark charges of the right-handed u and d quark fields.

$C_u^V = \frac{e(3\cos\tau - 8\sin^2\theta_W \cos\tau - 5\sin\theta_W \sin\tau \tan\epsilon)}{12\sin\theta_W \cos\theta_W} + \frac{g_D(3u+d)\sec\epsilon\sin\tau}{4}$
$C_u^A = -\frac{e(\cos\tau + \sin\theta_W \sin\tau\tan\epsilon)}{4\sin\theta_W\cos\theta_W} - \frac{g_D(d-u)\sec\epsilon\sin\tau}{4}$
$C_d^V = -\frac{e(3\cos\tau - 4\sin^2\theta_W \cos\tau - \sin\theta_W \sin\tau\tan\epsilon)}{12\sin\theta_W\cos\theta_W} + \frac{g_D(u+3d)\sec\epsilon\sin\tau}{4}$
$C_d^A = \frac{e(\cos\tau + \sin\tau\tan\epsilon)}{4\sin\theta_W\cos\theta_W} + \frac{g_D(d-u)\sec\epsilon\sin\tau}{4}$
$C_e^V = -\frac{e(\cos\tau - 4\sin^2\theta_W\cos\tau - \sin\theta_W\sin\tau\tan\epsilon)}{4\sin\theta_W\cos\theta_W} - \frac{g_D(7u+5d)\sec\epsilon\sin\tau}{4}$
$C_e^A = \frac{e(\cos\tau + \sin\theta_W\sin\tau\tan\epsilon)}{4\sin\theta_W\cos\theta_W} + \frac{g_D(d-u)\sec\epsilon\sin\tau}{4}$
$C_\nu^V = \frac{e(\cos\tau + \sin\theta_W\sin\tau\tan\epsilon)}{4\sin\theta_W\cos\theta_W} - \frac{g_D(5u+7d)\sec\epsilon\sin\tau}{4}$
$C_\nu^A = -\frac{e(\cos\tau + \sin\theta_W\sin\tau\tan\epsilon)}{4\sin\theta_W\cos\theta_W} - \frac{g_D(d-u)\sec\epsilon\sin\tau}{4}$

Table 3.4: Vector and axial couplings of fermions to A' boson. Here u and d are the free dark charges of the right-handed u and d quark fields.

$\varepsilon_u^V = -\frac{e(3\sin\tau - 8\sin^2\theta_W \sin\tau + 5\sin\theta_W \cos\tau \tan\epsilon)}{12\sin\theta_W \cos\theta_W} + \frac{g_D(3u+d)\cos\tau\sec\epsilon}{4}$
$\varepsilon_u^A = \frac{e(\sin\tau - \sin\theta_W \cos\tau\tan\epsilon)}{4\sin\theta_W\cos\theta_W} + \frac{g_D(u-d)\cos\tau\sec\epsilon}{4}$
$\varepsilon_d^V = \frac{e(3\sin\tau - 4\sin^2\theta_W \sin\tau + \sin\theta_W \cos\tau\tan\epsilon)}{12\sin\theta_W\cos\theta_W} + \frac{g_D(u+3d)\cos\tau\sec\epsilon}{4}$
$\varepsilon_d^A = -\frac{e(\sin\tau - \sin\theta_W \cos\tau\tan\epsilon)}{4\sin\theta_W\cos\theta_W} - \frac{g_D(u-d)\cos\tau\sec\epsilon}{4}$
$\varepsilon_e^V = \frac{e(\sin\tau - 4\sin^2\theta_W \sin\tau + 3\sin\theta_W \cos\tau\tan\epsilon)}{4\sin\theta_W\cos\theta_W} - \frac{g_D(7u+5d)\cos\tau\sec\epsilon}{4}$
$\varepsilon_e^A = -\frac{e(\sin\tau - \sin\theta_W \cos\tau\tan\epsilon)}{4\sin\theta_W\cos\theta_W} - \frac{g_D(u-d)\cos\tau\sec\epsilon}{4}$
$\varepsilon_\nu^V = -\frac{e(\sin\tau - \sin\theta_W \cos\tau\tan\epsilon)}{4\sin\theta_W\cos\theta_W} - \frac{g_D(5u+7d)\cos\tau\sec\epsilon}{4}$
$\varepsilon_\nu^A = \frac{e(\sin\tau - \sin\theta_W \cos\tau\tan\epsilon)}{4\sin\theta_W\cos\theta_W} + \frac{g_D(u-d)\cos\tau\sec\epsilon}{4}$

CHAPTER 4

THE ATOMKI EXPERIMENT AND OTHER CONSTRAINTS

Searching for heavier particles around 9 MeV was the idea of Boer and van Dantzig [37], [38]. They began their investigation using an e^+e^- spectrometer at the University of Frankfurt and conducted a series of experiments till the spectrometer was shutdown [39], [40]. After the shutdown, it was relocated to the ATOMKI accelerator facilities in Debrecen, Hungary [4]. The ATOMKI collaboration subsequently upgraded the spectrometer, enhancing its sensitivity, and have since conducted experiments involving ^{8}Be [6][41], ^{4}He [9] [10] and ^{12}C [11] nuclei. In the experiment, a target nucleus is excited by using the proton capture process. The excited nucleus then decays into a lower energy state by releasing an electron-positron pair. This process is called internal pair creation or conversion (IPC). The spectrometer used in the 2016 experiment can be seen in Figure 4.2, and the process is pictured in Figure 4.1. In 2016, decay of excited ^{8}Be was observed, and the collaboration announced that they found a notable bump in the distribution of the opening angles and invariant masses of e^+e^- pairs [6], illustrated in Figure 4.3. They reported a deviation of 6.8σ. Despite subsequent improvements to the experiment, the anomaly persisted, consistently showing deviations exceeding 6σ.

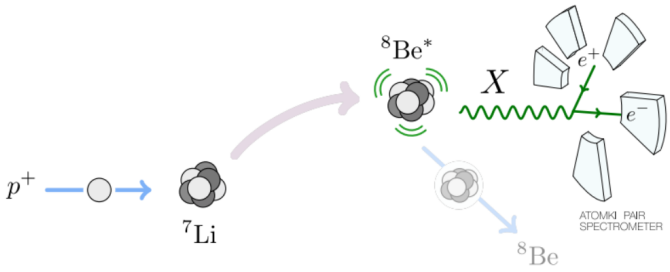

Figure 4.1: Simple illustration of the ATOMKI experiment [3].

Figure 4.2: The ATOMKI spectrometer used in 2016 measurement [4].

Since 2016, there has been no independent verification of the observed anomaly, raising concerns about its reliability. Although this anomaly was only observed in the Hungarian experiment, there are compelling reasons to believe it may be an authentic effect [4]:

- Observed standard deviation is always greater than 6σ.
- The set-up was improved from five arms to six. Nevertheless, the anomaly was observed anyway.
- They have used different position-sensitive detectors, but the anomaly didn't disappear.
- The anomaly was also observed with different proton beam energies as seen in Figure 4.3.
- The bumps show up at different angles with ^{8}Be and ^{4}He. Nevertheless, it is consistent with the theoretical expectation of 17 MeV particles. See Figure 4.4.
- No anomaly was observed with calibration atoms.

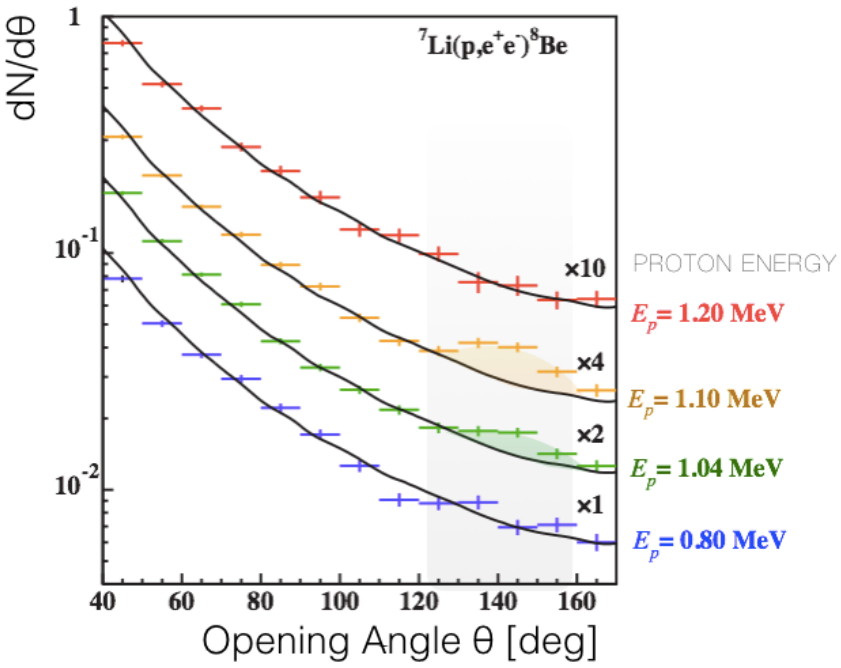

Figure 4.3: Bumps in the angular correlation of e^+e^- pairs at different proton energies. This figure is taken from [5], which is adapted from [6].

- No anomaly was observed in events when the momentum of e^+e^- pairs is not symmetric.

Thus, the chances of the anomaly being just a systematic error are not high.

In the ATOMKI experiment, angular correlations of electron-positron pairs from the decay of beryllium atoms with excitation energies 17.6 MeV (isovector transition) and 18.15 MeV (isoscalar transition) are observed ($J^\pi = 1^+ \to 0^+$). The unexpected bump was observed in the 18.15 MeV resonance.

Best fit to X particle mass is 17.01(16) MeV and the branching ratios compared to the γ-decay is [42]

$$\frac{Br(^8\text{Be}^* \to X + {}^8\text{Be})}{Br(^8\text{Be}^* \to \gamma\ {}^8\text{Be})} \times Br(X \to e^+e^-) = 6(1) \times 10^{-6}. \tag{4.1}$$

If the X boson couples to the current $J_\mu = \varepsilon_p \bar{p}\gamma^\mu p + \varepsilon_n \bar{n}\gamma^\mu n$, where $\varepsilon_p = 2\varepsilon_u + \varepsilon_d$ and $\varepsilon_n = \varepsilon_u + 2\varepsilon_d$, with the NA48 data (equation 4.4) the ratio between the neutron and proton is found,

$$-0.09 < \varepsilon_p/\varepsilon_n < 0.11 \tag{4.2}$$

when m_X is taken 17 MeV. This condition indicates the photophobic nature of the X boson. Even though the axial vector scenario is also considered a possible solution to the problem, there are significant uncertainties in the nuclear matrix elements that make it challenging to calculate the desired couplings.

The X boson decays to electron-positron pairs before it leaves the detectors; therefore, it gives a lower bound to electron coupling,

$$|\varepsilon_e^V| \gtrsim 1.3 \times 10^{-5} \sqrt{Br(X \to e^+e^-)} \tag{4.3}$$

Although the X boson can decay to $\nu\bar{\nu}$ and $\gamma\gamma\gamma$ assuming no other invisible decay channels, the decay to photons is negligible, and to neutrinos are assumed to be highly suppressed. Therefore, the branching ratio $Br(X \to e^+e^-)$ is assumed to be unity.

This unknown X particle can be a vector, an axial vector or a pseudoscalar mediator. But it cannot be a scalar particle. In the scalar case, the initial state is parity-even ^{8}Be*$\to^8$Be + X : $1^+ \to 0^+0^+$, but considering the angular momentum conservation final state turns out to be parity-odd. Due to parity conservation, the scalar case is excluded. The pseudoscalar scenario is excluded by experiments [43].

Currently, the anomaly has only been observed at the ATOMKI facilities, making independent confirmation of the X17 boson [1] crucial. At a 2023 workshop [4], new experiments aimed at observing X17 particles were discussed. These efforts seek first to replicate and then to enhance the ATOMKI experiment. The MEGII collaboration claims they can improve the geometric acceptance and the invariant mass resolution. Another experiment, under construction at the Czech Technical University in Prague, involves a spectrometric system based on a time projection chamber. Additionally, the n_TOF facility at CERN proposes to investigate the X17 boson through a neutron-induced reaction. Lastly, the INFN Legnaro National Laboratories have proposed a cost-effective design to repeat the Hungarian experiment, expecting to detect electron-positron pairs with kinetic energies reaching up to 20 MeV and an angular resolution of under one degree.

[1] A X boson with 17 MeV mass is sometimes called $X17$.

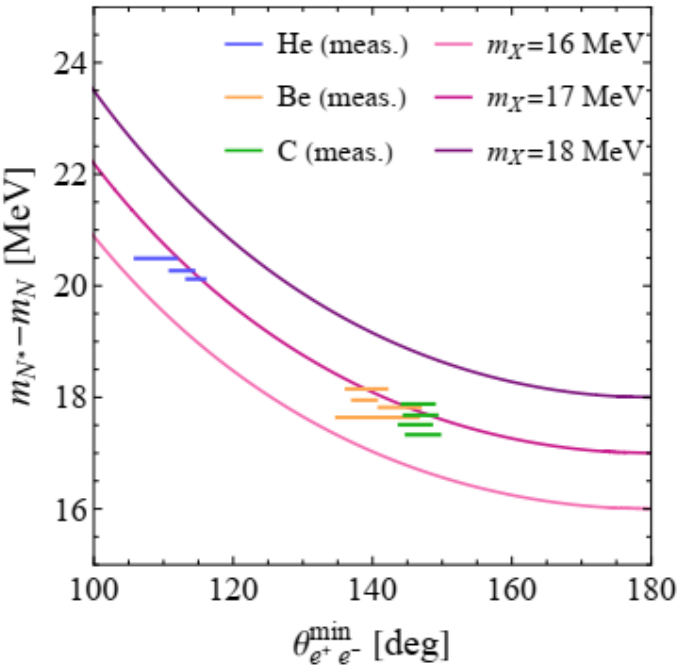

Figure 4.4: Contours are obtained by the relation $\theta^{min}_{e^+e^-} \approx 2\arcsin(m_X/(m_{N^*}-m_N))$ where $N^* \to NX$ [7]. Retrieved from [8].

4.1 Constraints from Other Experiments

To make a comprehensive analysis of the X17 particle, the constraints from other experiments need to be considered. Constraints listed below are taken from [44] and [3].

- The most confining constraint to quark couplings comes from neutral pion decay. The NA48/2 [45] experiment observes the rare pion decay, $\pi^0 \to \gamma X$. For the following decay $X \to e^+e^-$ this experiment gives the strongest bound [3]:

$$|2\varepsilon_u + \varepsilon_d| = |\varepsilon_p| \lesssim \frac{1.2 \times 10^{-3}}{\sqrt{Br(X \to e^+e^-)}}\,. \tag{4.4}$$

- NA64 [46] the beam dump experiment has established a lower bound on the electron coupling constant:

$$\sqrt{(\varepsilon_e^V)^2 + (\varepsilon_e^A)^2} \gtrsim 3.6 \times 10^{-5} \times \sqrt{Br(X \to e^+e^-)}. \tag{4.5}$$

- The upper bound to electron coupling comes from the KLOE experiment [47]:

$$\sqrt{(\varepsilon_e^V)^2 + (\varepsilon_e^A)^2} \lesssim 6.1 \times 10^{-4} / \sqrt{Br(X \to e^+e^-)}. \tag{4.6}$$

  If the electron coupling is lower, the X particle will escape the detector before decaying to an electron-positron pair [48]. However, a study [49] suggests that the nonexistence of electromagnetic signals from the decay of an X particle near the surface of a supernova progenitor star imposes stringent limits on the electron coupling constant. This leads to $|\varepsilon_e| < 10^{-12}/\sqrt{Br(X \to e^+e^-)}$ [8] implying another potential region for electron coupling constant.

- Moller scattering puts a boundary on the product of the vector and axial part of the electron. Measurements from SLAC E158 [50] give the following bounds [51]:

$$\left|\varepsilon_e^V \times \varepsilon_e^A\right| \lesssim 10^{-8}. \tag{4.7}$$

- TEXONO [52] constraints the electron and neutrino couplings in the following way [3]:

$$\begin{aligned} \sqrt{\left|\varepsilon_e^V \varepsilon_{\nu_e}^V\right|} &< 7 \times 10^{-5}, \quad \text{for } \varepsilon_e^V \varepsilon_\nu^V > 0 \\ \sqrt{\left|\varepsilon_e^V \varepsilon_{\nu_e}^V\right|} &< 3 \times 10^{-4}, \quad \text{for } \varepsilon_e^V \varepsilon_\nu^V < 0. \end{aligned} \tag{4.8}$$

  First line for constructive interference and second line for destructive interference scenario.

- Atomic parity violation observed in $^{133}_{55}$Cs [53] atoms with SM prediction [54] [55] gives a constraint in the following form:

$$\left|\varepsilon_e^A\right| \left|\frac{188}{399}\varepsilon_u^V + \frac{211}{399}\varepsilon_d^V\right| \lesssim 1.8 \times 10^{-12}\,. \tag{4.9}$$

4.2 Numerical Analysis

In this section, the constraints will be checked to determine if the unknown X particle can be the A' boson that was introduced in Chapter 3.

The first constraint on the unknown X particle is that it has a mass of around 17 MeV. Therefore, any model proposed to explain the anomaly must first satisfy this mass

requirement. A Stueckelberg mass was introduced in our model to provide additional flexibility within the theory. If desired, it can be simply set to zero, and the value of g_D will be solely determined by v_s and the dark charge assignment. It was observed that the graphs are insensitive to the values of $\tan\beta$ and $\sin\epsilon$. The behaviour of the graphs remains unchanged regardless of these values. Additionally, it can be observed that the largest possible g_D value is achieved when v_s takes the smallest value.

Ultimately, we have demonstrated that we can achieve the desired mass value with various combinations of charge assignments, v_s and g_D values. In Figure 4.5, graphs of v_s vs g_D are plotted. The effects of different model charges and the singlet vev can be inferred from the graphs.

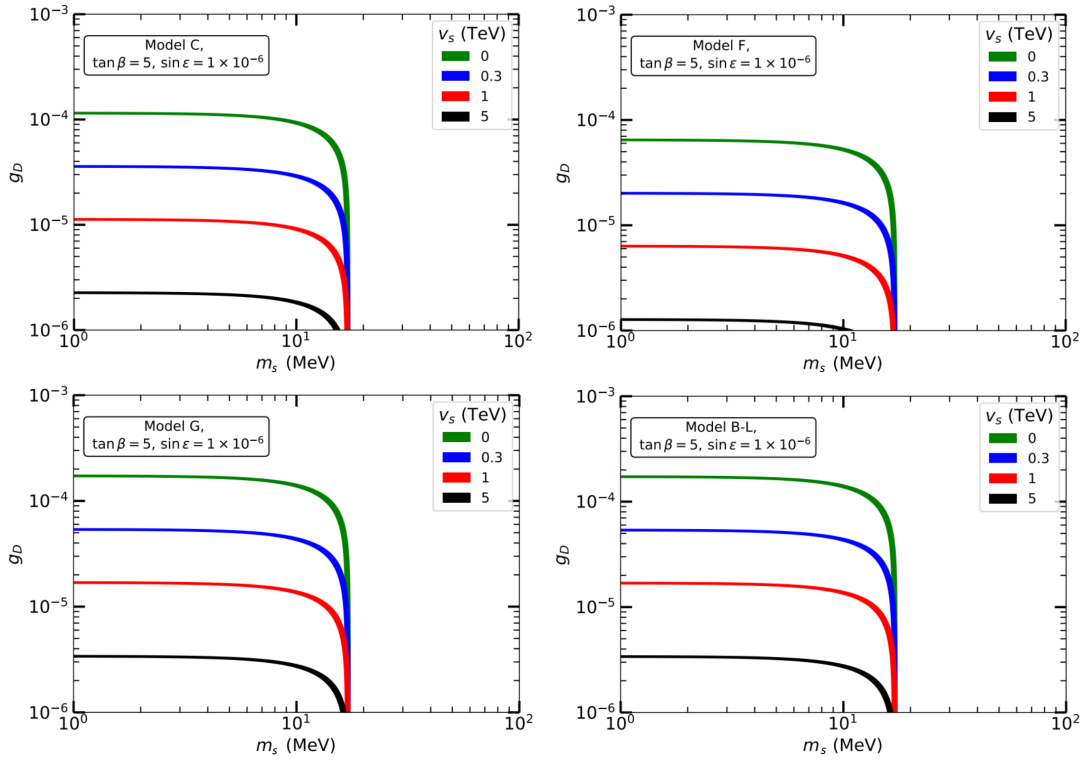

Figure 4.5: The dark photon mass in the Stueckelberg mass and the dark coupling parameter g_D plane for various models and singlet vev choices. In each curve, the dark photon mass $m_{A'} = 17$ MeV is demanded.

After it is determined that the desired mass value can be achieved for the A' particle, other constraints on the couplings must be checked. For this purpose, constraints from Section 4.1 are plotted in the following graphs. The part of the A'-fermion-

fermion couplings proportional to g_D, as shown in Table 3.4, is observed to be the dominant part of the equation. Consequently, the graphs are found to be scale invariant for almost all cases considered. In the following logarithmic plots (both axes are logarithmic), any g_D value in the power of ten will just repeat the same pattern. For this reason, the dark charge axes are multiplied by g_D, introducing redefined free dark charges, $\tilde{u} \equiv u\, g_D$ and $\tilde{d} \equiv d\, g_D$. Clearly, this redefinition can be made because g_D and dark charges always appear together in the same terms in equation 3.4, and due to scale invariance, one variable is reduced in the plots. Additionally, no significant dependence on $\tan\beta$ is observed. Values of $\tan\beta$ = 2, 10, & 50 are checked, and each result in the exact same graph in the chosen values of the other parameters. This can be seen in Figure 4.7 and Figure 4.8.

Looking at the graphs from Figure 4.7 to Figure 4.14, it is observed that the allowed mass region is larger for small v_s values. Apart from the mass region, v_s does not have a significant effect on other constraints. The atomic parity conservation constraints cover a larger area for smaller $\sin\epsilon$ values. For values of $\sin\epsilon$ bigger than 10^{-3}, the region disappears from the graphs. The $\sin\epsilon$ value also appears to determine the placement of the neutron-proton coupling ratio region. However, even though overlapping areas can be observed in other regions, this neutron-proton ratio does not coincide with the electron coupling region in any scenario studied. The atomic parity constraint is also very restrictive, and it coincides with other regions only in very small areas.

Searching through the parameter space and finding an overlapping area for all the regions may be possible, but chances appear to be remote based on the analysis conducted.

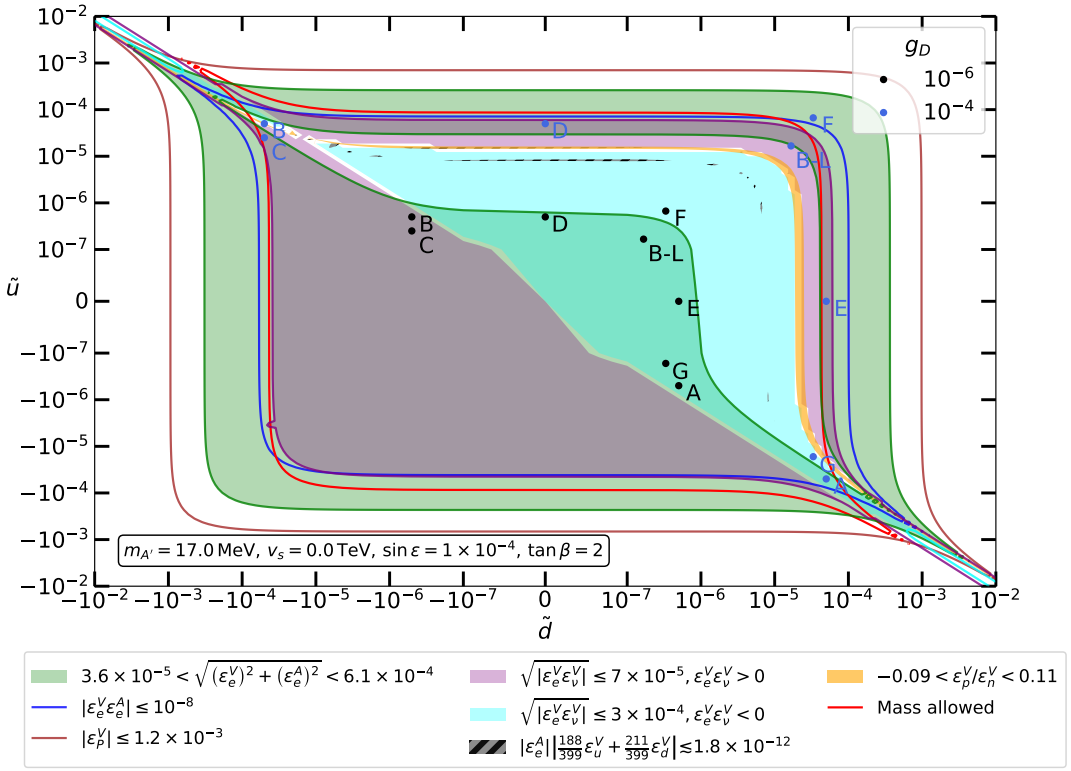

Figure 4.6: The allowed regions by various data in the plane of the redefined dark charges $\tilde{u} = ug_D$ and $\tilde{d} = dg_D$ for the dark photon A'. The region interior to the red, blue and brown lines represents the allowed parameter spaces for the mass, product of vector and axial couplings of the electron, and the proton couplings, respectively. The green-shaded region, outlined at its boundaries, defines the allowed region for electron coupling. The purple region outlined only at its outer boundary, along with the blue region with no outlines, represent the allowed region for electron and neutrino couplings in the constructive and destructive interference scenarios, respectively. The grey dashed area indicates the region where the atomic parity constraint is satisfied. Finally, the orange area corresponds to the ratio of proton to neutron couplings. The various fat dots on the graph correspond to the model points listed in Table 3.2, the charges multiplied by g_D value which are chosen 10^{-6} and 10^{-4} for the black and blue dots, respectively. In this graph, vev of the singlet is set to zero, the mixing parameter is $\sin\epsilon = 10^{-4}$, and the ratio between vevs of the Higgs doublets is $\tan\beta = 2$.

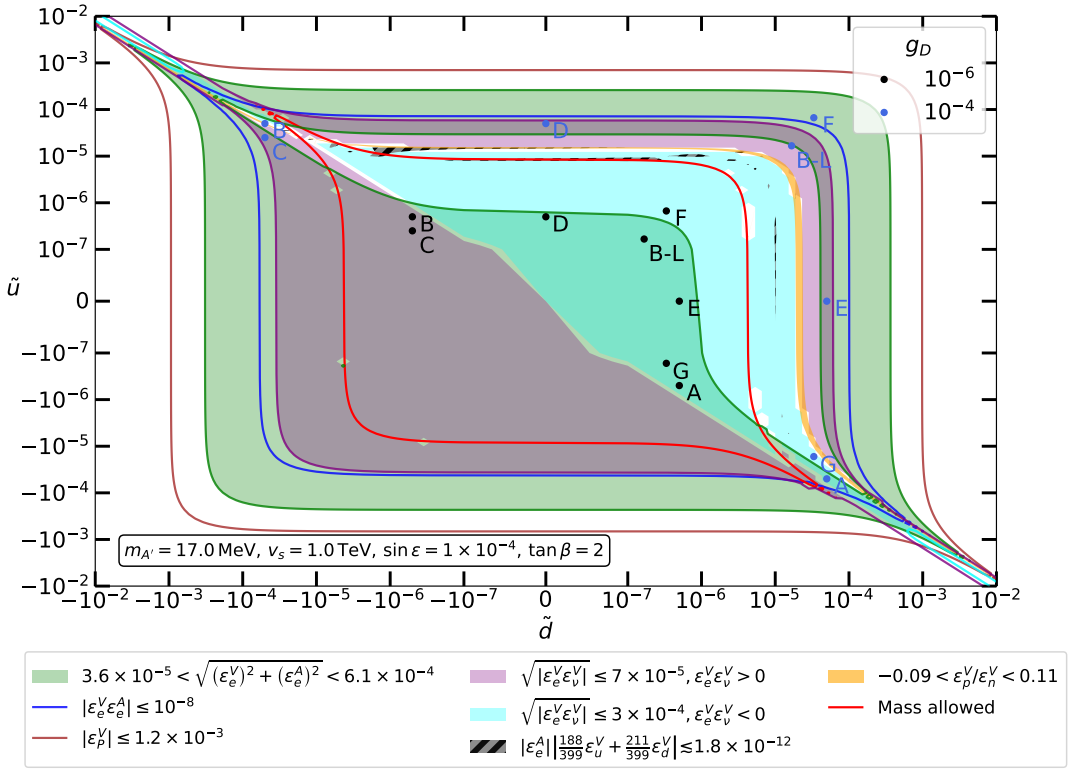

Figure 4.7: The allowed regions by various data in the plane of the redefined dark charges $\tilde{u} = ug_D$ and $\tilde{d} = dg_D$ for the dark photon A'. The region interior to the red, blue and brown lines represents the allowed parameter spaces for the mass, product of vector and axial couplings of the electron, and the proton couplings, respectively. The green-shaded region, outlined at its boundaries, defines the allowed region for electron coupling. The purple region outlined only at its outer boundary, along with the blue region with no outlines, represent the allowed region for electron and neutrino couplings in the constructive and destructive interference scenarios, respectively. The grey dashed area indicates the region where the atomic parity constraint is satisfied. Finally, the orange area corresponds to the ratio of proton to neutron couplings. The various fat dots on the graph correspond to the model points listed in Table 3.2, the charges multiplied by g_D value which are chosen 10^{-6} and 10^{-4} for the black and blue dots, respectively. In this graph, vev of the singlet is set to 1 TeV, the mixing parameter is $\sin\epsilon = 10^{-4}$, and the ratio between vevs of the Higgs doublets is $\tan\beta = 2$.

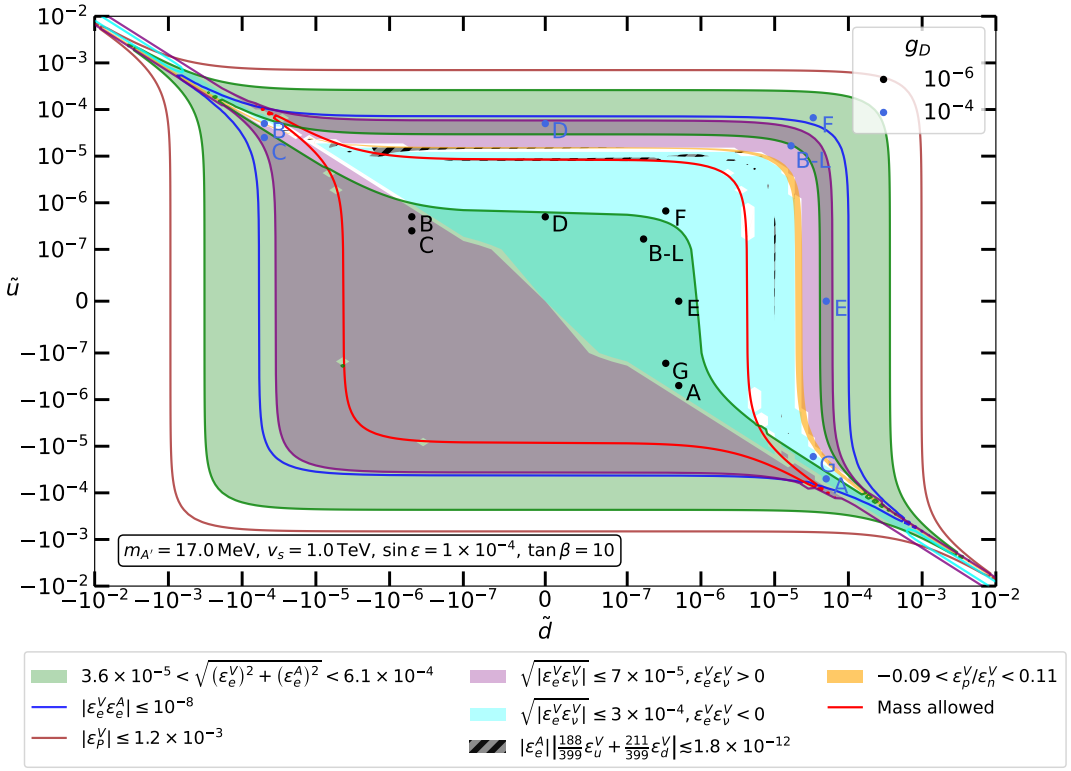

Figure 4.8: The allowed regions by various data in the plane of the redefined dark charges $\tilde{u} = ug_D$ and $\tilde{d} = dg_D$ for the dark photon A'. The region interior to the red, blue and brown lines represents the allowed parameter spaces for the mass, product of vector and axial couplings of the electron, and the proton couplings, respectively. The green-shaded region, outlined at its boundaries, defines the allowed region for electron coupling. The purple region outlined only at its outer boundary, along with the blue region with no outlines, represent the allowed region for electron and neutrino couplings in the constructive and destructive interference scenarios, respectively. The grey dashed area indicates the region where the atomic parity constraint is satisfied. Finally, the orange area corresponds to the ratio of proton to neutron couplings. The various fat dots on the graph correspond to the model points listed in Table 3.2, the charges multiplied by g_D value which are chosen 10^{-6} and 10^{-4} for the black and blue dots, respectively. In this graph, vev of the singlet is set to 1 TeV, the mixing parameter is $\sin\epsilon = 10^{-4}$, and the ratio between vevs of the Higgs doublets is $\tan\beta = 10$.

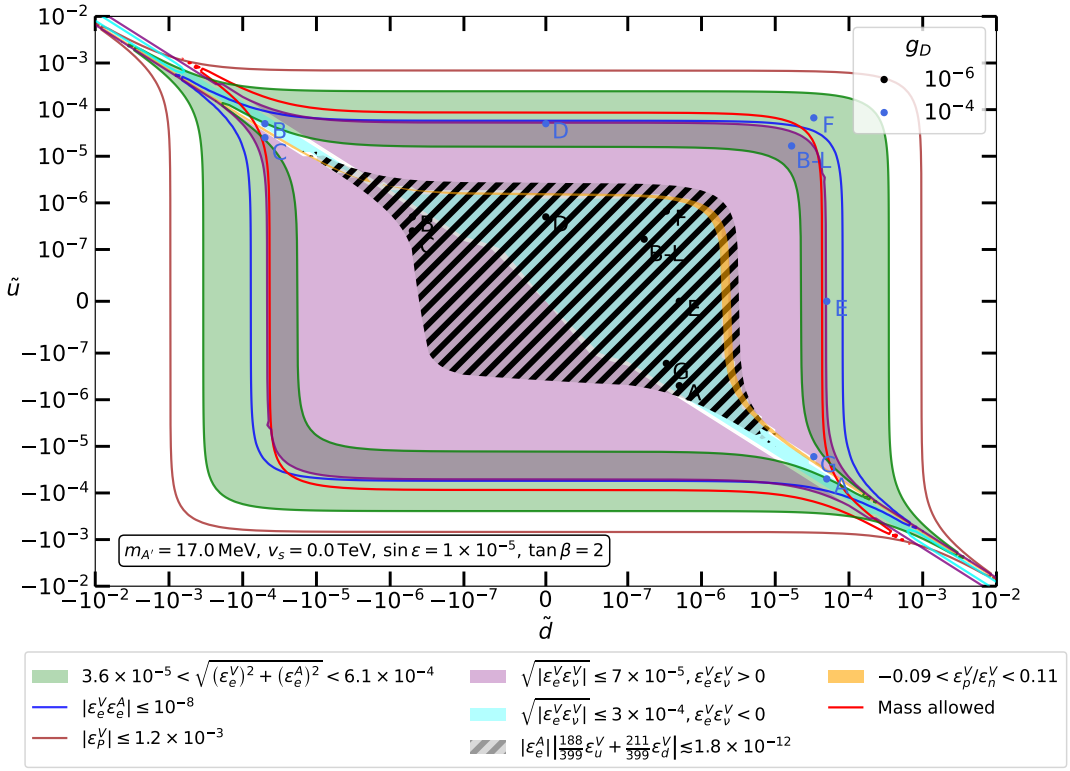

Figure 4.9: The allowed regions by various data in the plane of the redefined dark charges $\tilde{u} = ug_D$ and $\tilde{d} = dg_D$ for the dark photon A'. The region interior to the red, blue and brown lines represents the allowed parameter spaces for the mass, product of vector and axial couplings of the electron, and the proton couplings, respectively. The green-shaded region, outlined at its boundaries, defines the allowed region for electron coupling. The purple region outlined only at its outer boundary, along with the blue region with no outlines, represent the allowed region for electron and neutrino couplings in the constructive and destructive interference scenarios, respectively. The grey dashed area indicates the region where the atomic parity constraint is satisfied. Finally, the orange area corresponds to the ratio of proton to neutron couplings. The various fat dots on the graph correspond to the model points listed in Table 3.2, the charges multiplied by g_D value which are chosen 10^{-6} and 10^{-4} for the black and blue dots, respectively. In this graph, vev of the singlet is set to zero, the mixing parameter is $\sin\epsilon = 10^{-5}$, and the ratio between vevs of the Higgs doublets is $\tan\beta = 2$.

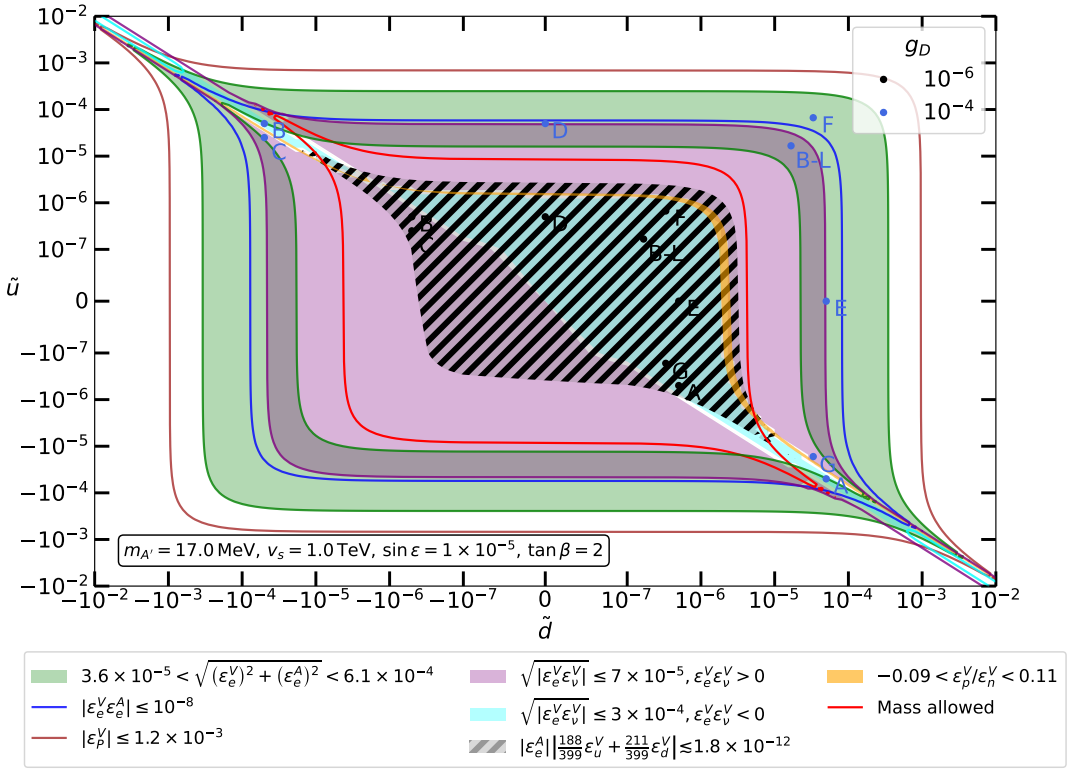

Figure 4.10: The allowed regions by various data in the plane of the redefined dark charges $\tilde{u} = ug_D$ and $\tilde{d} = dg_D$ for the dark photon A'. The region interior to the red, blue and brown lines represents the allowed parameter spaces for the mass, product of vector and axial couplings of the electron, and the proton couplings, respectively. The green-shaded region, outlined at its boundaries, defines the allowed region for electron coupling. The purple region outlined only at its outer boundary, along with the blue region with no outlines, represent the allowed region for electron and neutrino couplings in the constructive and destructive interference scenarios, respectively. The grey dashed area indicates the region where the atomic parity constraint is satisfied. Finally, the orange area corresponds to the ratio of proton to neutron couplings. The various fat dots on the graph correspond to the model points listed in Table 3.2, the charges multiplied by g_D value which are chosen 10^{-6} and 10^{-4} for the black and blue dots, respectively. In this graph, vev of the singlet is set to 1 TeV, the mixing parameter is $\sin\epsilon = 10^{-5}$, and the ratio between vevs of the Higgs doublets is $\tan\beta = 2$.

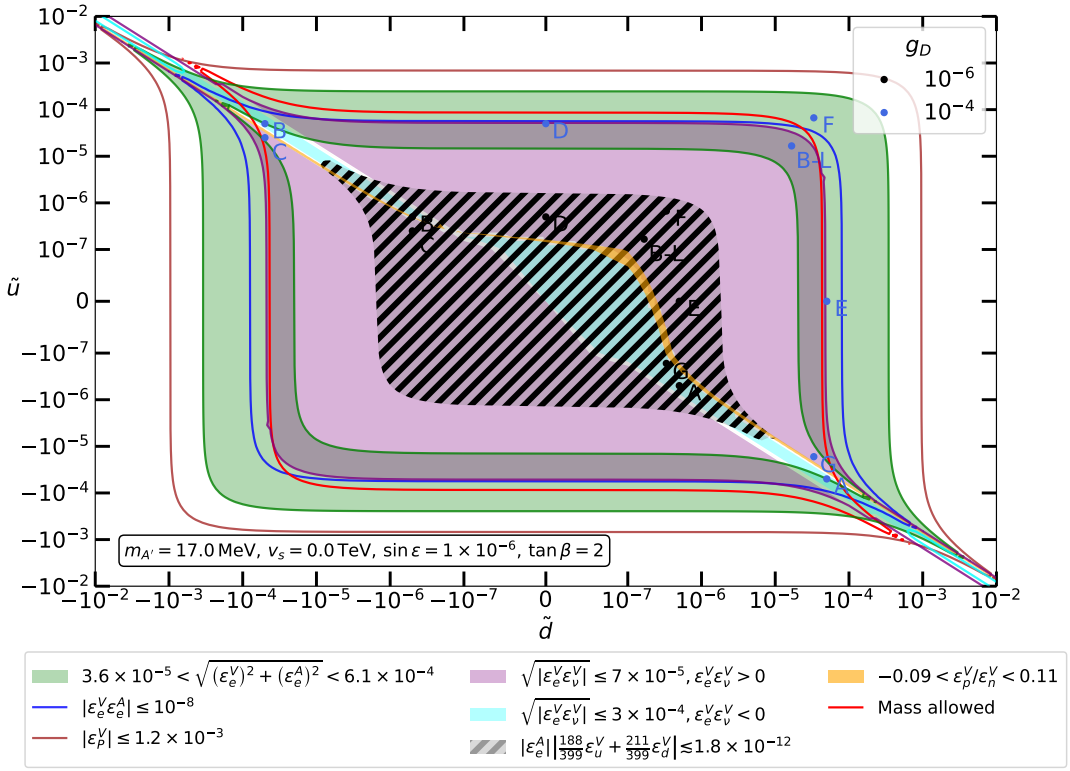

Figure 4.11: The allowed regions by various data in the plane of the redefined dark charges $\tilde{u} = ug_D$ and $\tilde{d} = dg_D$ for the dark photon A'. The region interior to the red, blue and brown lines represents the allowed parameter spaces for the mass, product of vector and axial couplings of the electron, and the proton couplings, respectively. The green-shaded region, outlined at its boundaries, defines the allowed region for electron coupling. The purple region outlined only at its outer boundary, along with the blue region with no outlines, represent the allowed region for electron and neutrino couplings in the constructive and destructive interference scenarios, respectively. The grey dashed area indicates the region where the atomic parity constraint is satisfied. Finally, the orange area corresponds to the ratio of proton to neutron couplings. The various fat dots on the graph correspond to the model points listed in Table 3.2, the charges multiplied by g_D value which are chosen 10^{-6} and 10^{-4} for the black and blue dots, respectively. In this graph, vev of the singlet is set to zero, the mixing parameter is $\sin\epsilon = 10^{-6}$, and the ratio between vevs of the Higgs doublets is $\tan\beta = 2$.

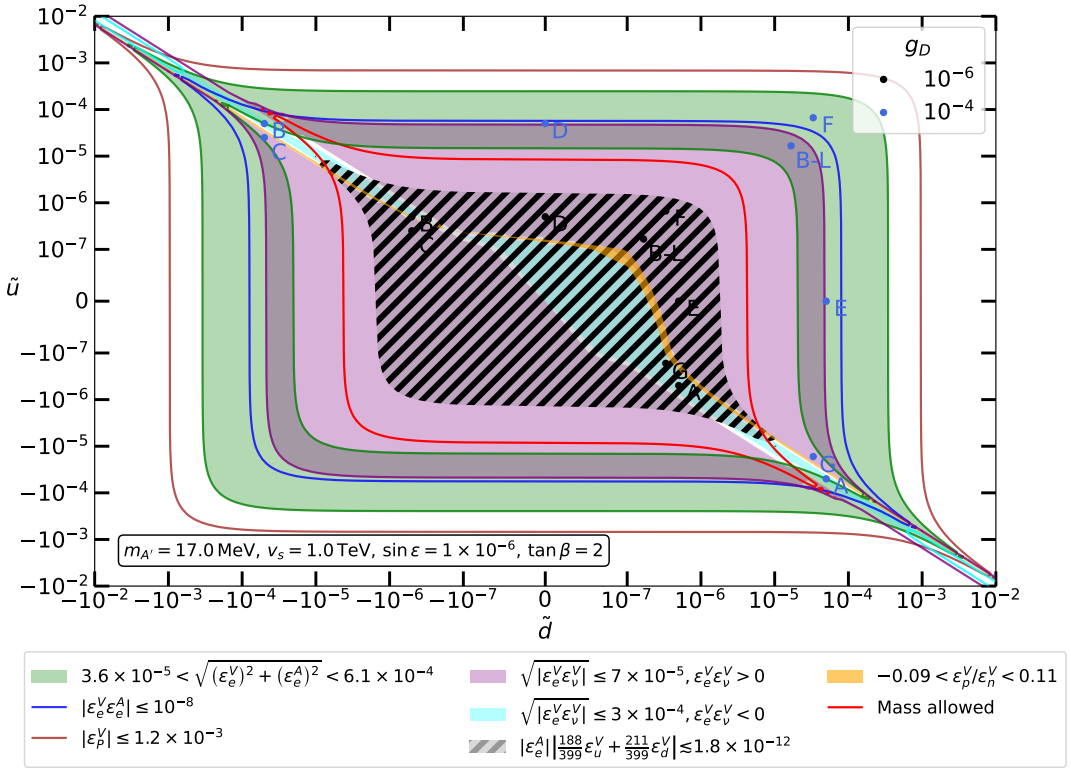

Figure 4.12: The allowed regions by various data in the plane of the redefined dark charges $\tilde{u} = ug_D$ and $\tilde{d} = dg_D$ for the dark photon A'. The region interior to the red, blue and brown lines represents the allowed parameter spaces for the mass, product of vector and axial couplings of the electron, and the proton couplings, respectively. The green-shaded region, outlined at its boundaries, defines the allowed region for electron coupling. The purple region outlined only at its outer boundary, along with the blue region with no outlines, represent the allowed region for electron and neutrino couplings in the constructive and destructive interference scenarios, respectively. The grey dashed area indicates the region where the atomic parity constraint is satisfied. Finally, the orange area corresponds to the ratio of proton to neutron couplings. The various fat dots on the graph correspond to the model points listed in Table 3.2, the charges multiplied by g_D value which are chosen 10^{-6} and 10^{-4} for the black and blue dots, respectively. In this graph, vev of the singlet is set to 1 TeV, the mixing parameter is $\sin\epsilon = 10^{-6}$, and the ratio between vevs of the Higgs doublets is $\tan\beta = 2$.

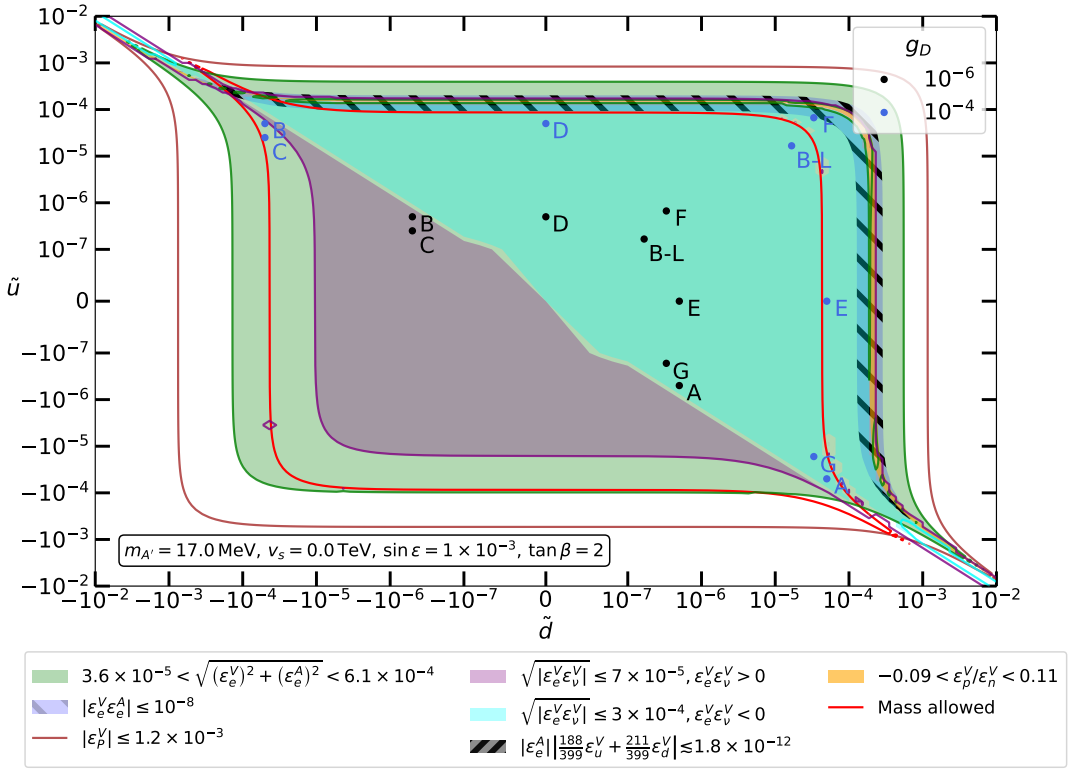

Figure 4.13: The allowed regions by various data in the plane of the redefined dark charges $\tilde{u} = ug_D$ and $\tilde{d} = dg_D$ for the dark photon A'. The region interior to the red and brown lines represents the allowed parameter spaces for the mass and the proton couplings, respectively. The green-shaded region, outlined at its boundaries, defines the allowed region for electron coupling. The dashed lavender-shaded region represents the allowed product of vector and axial couplings of the electron. The purple region outlined only at its outer boundary, along with the blue region with no outlines, represent the allowed region for electron and neutrino couplings in the constructive and destructive interference scenarios, respectively. The grey dashed area indicates the region where the atomic parity constraint is satisfied. Finally, the orange area corresponds to the ratio of proton to neutron couplings. The various fat dots on the graph correspond to the model points listed in Table 3.2, the charges multiplied by g_D value which are chosen 10^{-6} and 10^{-4} for the black and blue dots, respectively. In this graph, vev of the singlet is set to zero, the mixing parameter is $\sin\epsilon = 10^{-3}$, and the ratio between vevs of the Higgs doublets is $\tan\beta = 2$.

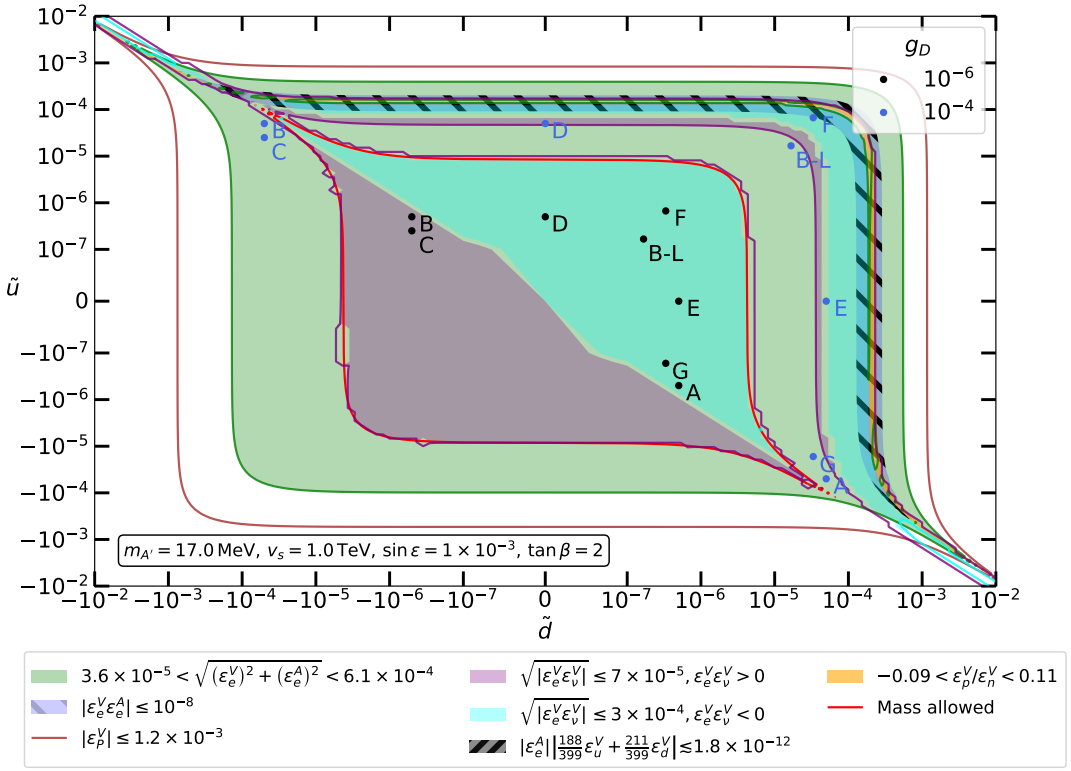

Figure 4.14: The allowed regions by various data in the plane of the redefined dark charges $\tilde{u} = ug_D$ and $\tilde{d} = dg_D$ for the dark photon A'. The region interior to the red and brown lines represents the allowed parameter spaces for the mass and the proton couplings, respectively. The green-shaded region, outlined at its boundaries, defines the allowed region for electron coupling. The dashed lavender-shaded region represents the allowed product of vector and axial couplings of the electron. The purple region outlined only at its outer boundary, along with the blue region with no outlines, represent the allowed region for electron and neutrino couplings in the constructive and destructive interference scenarios, respectively. The grey dashed area indicates the region where the atomic parity constraint is satisfied. Finally, the orange area corresponds to the ratio of proton to neutron couplings. The various fat dots on the graph correspond to the model points listed in Table 3.2, the charges multiplied by g_D value which are chosen 10^{-6} and 10^{-4} for the black and blue dots, respectively. In this graph, vev of the singlet is set to 1 TeV, the mixing parameter is $\sin\epsilon = 10^{-3}$, and the ratio between vevs of the Higgs doublets is $\tan\beta = 2$.

CHAPTER 5

CONCLUSIONS

In 2016, the ATOMKI collaboration observed an anomaly with a high significance. Since then, their set-up has been improved, and the experiment has been repeated, with the anomaly continuing to be observed. The anomaly suggests the possible existence of a 17 MeV boson. Although independent verification of the anomaly has not yet been achieved, there are reasons to believe that what has been observed is a genuine effect. Various attempts to replicate the experiment are ongoing; if confirmed, this observation would be a big step forward for BSM physics.

In this thesis, an extended 2HDM model is scrutinised. The observed X17 particle is explained through the introduction of a new Abelian gauge symmetry, with a second Higgs doublet and a new singlet implemented into the SM. The model also includes a Stueckelberg mass term to provide additional freedom in the model. The experimental data is very constraining, resulting in the exclusion of a large area for the coupling constants. However, the allowed region has been significantly widened by the introduction of the Stueckelberg term. Nevertheless, no overlapping area for all the constraints was observed. The tension is not high and is primarily between the electron coupling and the ratio of proton-neutron couplings.

Comparing the theory with the experiments, some challenges are encountered. First, the nuclear matrix element for the axial vector case has large uncertainties. To enable more sensitive analyses, further study of the axial nuclear matrix element is required. Second, throughout the analyses, the X boson was assumed to decay only to electron-proton pairs. Therefore, to improve the sensitivity of the analysis, other decay channels should be considered.

In this thesis, only the beryllium case is studied, but the ATOMKI collaboration observed the anomaly in both the helium and carbon decays. These cases can be explored in further research.

REFERENCES

[1] M. D. Campos, D. Cogollo, M. Lindner, T. Melo, F. S. Queiroz, and W. Rodejohann, "Neutrino masses and absence of flavor changing interactions in the 2HDM from gauge principles," *Journal of High Energy Physics*, vol. 2017, no. 8, pp. 1–49, 2017.

[2] A. Elpe, E. Akyumuk, T. Aliev, L. Selbuz, and I. Turan, "Constraining non-minimal dark sector scenarios with the COHERENT neutrino scattering data," *Physical Review D*, vol. 107, no. 7, p. 075022, 2023.

[3] J. L. Feng, B. Fornal, I. Galon, S. Gardner, J. Smolinsky, T. M. Tait, and P. Tanedo, "Particle physics models for the 17 MeV anomaly in beryllium nuclear decays," *Physical Review D*, vol. 95, no. 3, p. 035017, 2017.

[4] D. S. M. Alves *et al.*, "Shedding light on X17: community report," *European Physical Journal C*, vol. 83, no. 3, p. 230, 2023.

[5] F. Tanedo, "The delirium over beryllium," 2016. `https://www.quantumdiaries.org/2016/08/25/the-delirium-over-beryllium/`.

[6] A. Krasznahorkay, M. Csatlós, L. Csige, Z. Gácsi, J. Gulyás, M. Hunyadi, I. Kuti, B. M. Nyakó, L. Stuhl, J. Timár, *et al.*, "Observation of anomalous internal pair creation in ^{8}Be: A possible indication of a light, neutral boson," *Physical Review Letters*, vol. 116, no. 4, p. 042501, 2016.

[7] J. L. Feng, T. M. Tait, and C. B. Verhaaren, "Dynamical evidence for a fifth force explanation of the ATOMKI nuclear anomalies," *Physical Review D*, vol. 102, no. 3, p. 036016, 2020.

[8] P. B. Denton and J. Gehrlein, "Neutrino constraints and the ATOMKI X17 anomaly," *Physical Review D*, vol. 108, no. 1, p. 015009, 2023.

[9] A. J. Krasznahorkay, M. Csatlos, L. Csige, J. Gulyas, M. Koszta, B. Szihalmi, J. Timar, D. S. Firak, A. Nagy, N. J. Sas, and A. Krasznahorkay, "New evidence supporting the existence of the hypothetic X17 particle," 2019. arXiv:1910.10459.

[10] A. Krasznahorkay, M. Csatlós, L. Csige, J. Gulyás, A. Krasznahorkay, B. Nyakó, I. Rajta, J. Timár, I. Vajda, and N. Sas, "New anomaly observed in ^{4}He supports the existence of the hypothetical X17 particle," *Physical Review C*, vol. 104, no. 4, p. 044003, 2021.

[11] A. Krasznahorkay, A. Krasznahorkay, M. Begala, M. Csatlós, L. Csige, J. Gulyás, A. Krakó, J. Timár, I. Rajta, I. Vajda, *et al.*, "New anomaly observed in ^{4}C supports the existence and the vector character of the hypothetical X17 boson," *Physical Review C*, vol. 106, no. 6, p. L061601, 2022.

[12] G. C. Branco, P. Ferreira, L. Lavoura, M. Rebelo, M. Sher, and J. P. Silva, "Theory and phenomenology of two-Higgs-doublet models," *Physics Reports*, vol. 516, no. 1-2, pp. 1–102, 2012.

[13] G. Kane, "The search for supersymmetry: Probing physics beyond the standard model," *Physics Reports (Review Section of Physics Letters)*, vol. 117, no. 2-4, pp. 75–263, 1985.

[14] B. Dasgupta, E. Ma, and K. Tsumura, "Weakly interacting massive particle dark matter and radiative neutrino mass from Peccei-Quinn symmetry," *Physical Review D*, vol. 89, p. 041702, 2014.

[15] R. D. Peccei and H. R. Quinn, "CP conservation in the presence of pseudoparticles," *Physical Review Letters*, vol. 38, pp. 1440–1443, 1977.

[16] M. Trodden, "Electroweak baryogenesis: A Brief review," in *33rd Rencontres de Moriond: Electroweak Interactions and Unified Theories*, pp. 471–480, 1998.

[17] S. L. Glashow, "Partial-symmetries of weak interactions," *Nuclear physics*, vol. 22, no. 4, pp. 579–588, 1961.

[18] P. W. Higgs, "Broken symmetries and the masses of gauge bosons," *Physical Review Letters*, vol. 13, no. 16, p. 508, 1964.

[19] S. Weinberg, "A model of leptons," *Physical Review Letters*, vol. 19, no. 21, p. 1264, 1967.

[20] A. Salam, "Elementary particle theory," in *Prog. Of the Nobel Symposium, 1968, Stockholm, Sweden*, vol. 367, 1968.

[21] M. E. Peskin and D. V. Schroeder, *An Introduction to Quantum Field Theory*. Westview Press, 1995.

[22] T. Lancaster and S. Blundell, *Quantum Field Theory for the Gifted Amateur*. OUP Oxford, 2014.

[23] Y. Nagashima, *Elementary Particle Physics: Foundations of the Standard Model V2*. Wiley, 2013.

[24] K. Nakamura, K. Hagiwara, K. Hikasa, H. Murayama, M. Tanabashi, T. Watari, C. Amsler, M. Antonelli, D. Asner, H. Baer, *et al.*, "Review of particle physics," *Journal of Physics G: Nuclear and Particle Physics*, vol. 37, no. 7 A, p. 075021, 2010.

[25] M. Sher, "Flavor-changing neutral currents in the Higgs sector," *Modern Physics Letters A*, vol. 37, no. 22, 2022.

[26] S. L. Glashow and S. Weinberg, "Natural conservation laws for neutral currents," *Physical Review D*, vol. 15, no. 7, p. 1958, 1977.

[27] P. Ko, Y. Omura, and C. Yu, "A resolution of the flavor problem of two Higgs doublet models with an extra $U(1)_H$ symmetry for Higgs flavor," *Physics Letters B*, vol. 717, no. 1-3, pp. 202–206, 2012.

[28] I. F. Ginzburg and M. Krawczyk, "Symmetries of two Higgs doublet model and CP violation," *Physical Review D—Particles, Fields, Gravitation, and Cosmology*, vol. 72, no. 11, p. 115013, 2005.

[29] P. M. Ferreira, B. Grzadkowski, O. M. Ogreid, and P. Osland, "Softly broken symmetries in the 2HDM—an invariant formulation," *Journal of High Energy Physics*, vol. 2023, no. 1, pp. 1–41, 2023.

[30] J. Schechter and J. W. F. Valle, "Neutrino masses in $SU(2) \bigotimes U(1)$ theories," *Physical Review D*, vol. 22, pp. 2227–2235, 1980.

[31] R. N. Mohapatra and G. Senjanović, "Neutrino mass and spontaneous parity nonconservation," *Physical Review Letters*, vol. 44, pp. 912–915, 1980.

[32] V. Brdar, A. J. Helmboldt, S. Iwamoto, and K. Schmitz, "Type I seesaw mechanism as the common origin of neutrino mass, baryon asymmetry, and the electroweak scale," *Physical Review D*, vol. 100, p. 075029, 2019.

[33] E. C. G. Stückelberg, "Interaction energy in electrodynamics and in the field theory of nuclear forces," *Helvetica Physica Acta*, vol. 11, no. 3, p. 225, 1938.

[34] B. Körs and P. Nath, "A Stueckelberg extension of the Standard Model," *Physics Letters B*, vol. 586, no. 3–4, p. 366–372, 2004.

[35] D. Feldman, Z. Liu, and P. Nath, "The Stueckelberg Z' extension with kinetic mixing and milli-charged dark matter from the hidden sector," *Physical Review D*, vol. 75, no. 11, 2007.

[36] G. Panotopoulos and P. Tuzón, "The physics of a new gauge boson in a Stueckelberg extension of the two-Higgs-doublet model," *Journal of High Energy Physics*, vol. 2011, no. 7, 2011.

[37] F. De Boer, O. Fröhlich, K. Stiebing, K. Bethge, H. Bokemeyer, A. Balanda, A. Buda, R. Van Dantzig, T. W. Elze, H. Folger, *et al.*, "A deviation in internal pair conversion," *Physics Letters B*, vol. 388, no. 2, pp. 235–240, 1996.

[38] F. W. N. de Boer and R. van Dantzig, "de Boer and van Dantzig reply," *Physical Review Letters*, vol. 62, pp. 2639–2639, 1989.

[39] F. De Boer, K. Bethge, H. Bokemeyer, R. van Dantzig, J. van Klinken, V. Mironov, K. Müller, and K. Stiebing, "Further search for a neutral boson with a mass around 9 MeV/c^2," *Journal of Physics G: Nuclear and Particle Physics*, vol. 27, no. 4, p. L29, 2001.

[40] K. Stiebing, F. de Boer, O. Fröhlich, H. Bokemeyer, K. Müller, K. Bethge, and J. van Klinken, "A multi-detector array for high energy nuclear e^+e^- pair spectroscopy," *Journal of Physics G: Nuclear and Particle Physics*, vol. 30, no. 2, p. 165, 2004.

[41] A. Krasznahorkay, M. Csatlós, L. Csige, Z. Gácsi, J. Gulyás, Á. Nagy, N. Sas, J. Tímár, T. Tornyi, and I. Vajda, "New results on the ^{8}Be anomaly," *Journal of Physics: Conference Series*, vol. 1056, no. 1, p. 012028, 2018.

[42] L. Csige, A. Krasznahorkay, M. Csatlós, D. Firak, J. Gulyás, Á. Nagy, N. Sas, J. Tímár, and T. G. Tornyi, "On the X(17) light-particle candidate observed in nuclear transitions," *Acta Physica Polonica B*, vol. 50, no. 3, pp. 675–684, 2019.

[43] J. L. Feng, B. Fornal, I. Galon, S. Gardner, J. Smolinsky, T. M. Tait, and P. Tanedo, "Protophobic fifth-force interpretation of the observed anomaly in ^{8}Be nuclear transitions," *Physical Review Letters*, vol. 117, no. 7, p. 071803, 2016.

[44] D. Barducci and C. Toni, "An updated view on the ATOMKI nuclear anomalies," *Journal of High Energy Physics*, vol. 2023, no. 2, pp. 1–46, 2023.

[45] M. Raggi, G. Anzivino, R. Arcidiacono, W. Baldini, S. Balev, J. Batley, M. Behler, S. Bifani, C. Biino, A. Bizzeti, *et al.*, "NA48/2 studies of rare decays," *Il Nuovo Cimento C*, vol. 38, pp. 1–9, 2015.

[46] D. Banerjee, J. Bernhard, V. E. Burtsev, A. G. Chumakov, D. Cooke, P. Crivelli, E. Depero, A. V. Dermenev, S. V. Donskov, R. R. Dusaev, T. Enik, N. Charitonidis, A. Feshchenko, V. N. Frolov, A. Gardikiotis, S. G. Gerassimov, S. N. Gninenko, M. Hösgen, M. Jeckel, V. A. Kachanov, A. E. Karneyeu, G. Kekelidze, B. Ketzer, D. V. Kirpichnikov, M. M. Kirsanov, V. N. Kolosov, I. V. Konorov, S. G. Kovalenko, V. A. Kramarenko, L. V. Kravchuk, N. V. Krasnikov, S. V. Kuleshov, V. E. Lyubovitskij, V. Lysan, V. A. Matveev, Y. V. Mikhailov, L. Molina Bueno, D. V. Peshekhonov, V. A. Polyakov, B. Radics, R. Rojas, A. Rubbia, V. D. Samoylenko, D. Shchukin, V. O. Tikhomirov, I. Tlisova, D. A. Tlisov, A. N. Toropin, A. Y. Trifonov, B. I. Vasilishin, G. Vasquez Arenas, P. V. Volkov, V. Y. Volkov, and P. Ulloa, "Improved limits on a hypothetical $X(16.7)$ boson and a dark photon decaying into e^+e^- pairs," *Physical Review D*, vol. 101, p. 071101, 2020.

[47] A. Anastasi, D. Babusci, G. Bencivenni, M. Berlowski, C. Bloise, F. Bossi, P. Branchini, A. Budano, L. C. Balkeståhl, B. Cao, *et al.*, "Limit on the pro-

duction of a low-mass vector boson in $e^+e^- \to \mathrm{u}\gamma$, $\mathrm{u} \to e^+e^-$ with the KLOE experiment," *Physics Letters B*, vol. 750, pp. 633–637, 2015.

[48] J. D. Bjorken, S. Ecklund, W. R. Nelson, A. Abashian, C. Church, B. Lu, L. W. Mo, T. A. Nunamaker, and P. Rassmann, "Search for neutral metastable penetrating particles produced in the SLAC beam dump," *Physical Review D*, vol. 38, pp. 3375–3386, 1988.

[49] D. Kazanas, R. N. Mohapatra, S. Nussinov, V. L. Teplitz, and Y. Zhang, "Supernova bounds on the dark photon using its electromagnetic decay," *Nuclear Physics B*, vol. 890, pp. 17–29, 2015.

[50] P. L. Anthony, R. G. Arnold, C. Arroyo, K. Bega, J. Biesiada, P. E. Bosted, G. Bower, J. Cahoon, R. Carr, G. D. Cates, J.-P. Chen, E. Chudakov, M. Cooke, P. Decowski, A. Deur, W. Emam, R. Erickson, T. Fieguth, C. Field, J. Gao, M. Gary, K. Gustafsson, R. S. Hicks, R. Holmes, E. W. Hughes, T. B. Humensky, G. M. Jones, L. J. Kaufman, L. Keller, Y. G. Kolomensky, K. S. Kumar, P. LaViolette, D. Lhuillier, R. M. Lombard-Nelsen, Z. Marshall, P. Mastromarino, R. D. McKeown, R. Michaels, J. Niedziela, M. Olson, K. D. Paschke, G. A. Peterson, R. Pitthan, D. Relyea, S. E. Rock, O. Saxton, J. Singh, P. A. Souder, Z. M. Szalata, J. Turner, B. Tweedie, A. Vacheret, D. Walz, T. Weber, J. Weisend, M. Woods, and I. Younus, "Precision measurement of the weak mixing angle in Møller scattering," *Physical Review Letters*, vol. 95, p. 081601, 2005.

[51] Y. Kahn, G. Krnjaic, S. Mishra-Sharma, and T. M. Tait, "Light weakly coupled axial forces: models, constraints, and projections," *Journal of High Energy Physics*, vol. 2017, no. 5, pp. 1–34, 2017.

[52] M. Deniz, S. T. Lin, V. Singh, J. Li, H. T. Wong, S. Bilmis, C. Y. Chang, H. M. Chang, W. C. Chang, C. P. Chen, M. H. Chou, K. J. Dong, J. M. Fang, C. H. Hu, G. C. Jon, W. S. Kuo, W. P. Lai, F. S. Lee, S. C. Lee, H. B. Li, H. Y. Liao, C. W. Lin, F. K. Lin, S. K. Lin, Y. Liu, J. F. Qiu, M. Serin, H. Y. Sheng, L. Singh, R. F. Su, W. S. Tong, J. J. Wang, P. L. Wang, S. C. Wu, S. W. Yang, C. X. Yu, Q. Yue, M. Zeyrek, D. X. Zhao, Z. Y. Zhou, Y. F. Zhu, and B. A. Zhuang, "Measurement of $\overline{\nu}_{\mathrm{e}}$-electron scattering cross section with a CsI(Tl) scintillating crystal array at

the Kuo-Sheng nuclear power reactor," *Physical Review D*, vol. 81, p. 072001, 2010.

[53] S. G. Porsev, K. Beloy, and A. Derevianko, "Precision determination of electroweak coupling from atomic parity violation and implications for particle physics," *Physical Review Letters*, vol. 102, p. 181601, 2009.

[54] V. A. Dzuba, J. C. Berengut, V. V. Flambaum, and B. Roberts, "Revisiting parity nonconservation in cesium," *Physical Review Letters*, vol. 109, p. 203003, 2012.

[55] G. Arcadi, M. Lindner, J. Martins, and F. S. Queiroz, "New physics probes: Atomic parity violation, polarized electron scattering and neutrino-nucleus coherent scattering," *Nuclear Physics B*, vol. 959, p. 115158, 2020.